MICROBIOLOGY AND MOLECULAR BIOLOGY REVIEWS, Dec. 2005, p. 665–695 Vol. 69, No. 4
1092-2172/05/$08.00+0 doi:10.1128/MMBR.69.4.665–695.2005

The 2-Hydroxycarboxylate Transporter Family: Physiology, Structure, and Mechanism

Iwona Sobczak† and Juke S. Lolkema*

Molecular Microbiology, Groningen Biomolecular Sciences and Biotechnology Institute, University of Groningen, Haren, The Netherlands

INTRODUCTION 665
FUNCTION 666
Distribution and Phylogeny 666
Transport Properties 668
Physiological Function 669
Malolactic fermentation 670
Genetic organization of malolactic fermentation genes 672
Oxidative malate decarboxylation pathway 672
Citrolactic fermentation 674
Citrate fermentation in the gamma subdivision of *Proteobacteria* 675
Distribution of citrate fermentation in the bacterial kingdom 675
Evolutionary states of energy coupling to oxaloacetate decarboxylases 678
PROTEINS 678
Cloning and Expression 678
Purification and Reconstitution 680
STRUCTURE 680
Primary Structure 680
Superfamilies and structural classes 680
Sequence analysis 681
Domain structure 681
Membrane Topology 682
Transmembrane segments 682
Amphipathic helix and membrane insertion 684
Pore-loop structure 685
Structural Model 685
Quaternary Structure 686
MECHANISMS 686
Kinetics 686
Symport and exchange 686
Antiport mechanism of CitS 688
Alternate access 688
Structure-Function Relationships 689
The conserved Arg in TMS XI 689
Chimeras of CitP and MleP 689
Interaction of substrate and co-ions with the Xa region 690
Mutations in the Vb region 691
Mechanistic Model 691
CONCLUSIONS 692
ACKNOWLEDGMENTS 692
REFERENCES 692

INTRODUCTION

Integral membrane proteins are present in all living organisms in large numbers. Many of these proteins are involved in transport processes that are essential for proper functioning of a living cell. In *Escherichia coli*, about 10% of all chromosomal genes code for transport proteins (103). According to the transport classification system (TC system) there are over 250 families of putative transport proteins, and the largest functional category is represented by 85 families of secondary transporters (17, 117; http://www.tcdb.org).

Secondary transporters use the free energy stored in ion and/or solute gradients across the membrane to drive transport. The transporters are commonly classified in three groups based on their mode of energy coupling: (i) uniporters catalyze

* Corresponding author. Mailing address: Molecular Microbiology, University of Groningen, Kerklaan 30, 9751 NN Haren, The Netherlands. Phone: 31 50 363 2155. Fax: 31 50 363 2154. E-mail: j.s.lolkema@biol.rug.nl.

† Present address: Analytical Biochemistry, University Centre for Pharmacy, University of Groningen, Postbus 196, 9700 AD Groningen, The Netherlands.

the translocation of a single solute across the membrane, (ii) symporters couple the translocation of a solute to the translocation of a co-ion(s) in the same direction, and (iii) antiporters couple the translocation of a solute and a co-ion(s) in opposite directions. Many antiporters couple the translocation of one solute to the translocation of another solute rather than a co-ion. They exchange a substrate at one side of the membrane for another substrate at the other side of the membrane. Symporters (and uniporters) can catalyze a similar reaction when they operate in the exchange mode of transport, a partial reaction. This exchange mode catalyzed by symporters differs from the antiport mechanism in that the translocations of the two substrates in the two directions are not obligatorily coupled. Symporters catalyzing exchange under physiological conditions are termed exchangers. The different modes of energy coupling enable transporters to play an important role in different aspects of the physiology of the cell. Thus, the symport and uniport mechanisms allow the cell to take up nutrients from the medium, while antiporters may function in the excretion of end products or in defense mechanisms by removing harmful compounds from the cell. Antiporters and exchangers may combine the uptake of a nutrient from the environment and the excretion of a metabolic end product.

As a rule, transport catalyzed by secondary transporters is a metabolic energy-requiring process. Symporters and antiporters couple the translocation of the substrate to the translocation of protons or sodium ions. The electrochemical gradients of H^+ and Na^+ across the membrane, or proton motive force (PMF) and sodium ion motive force, respectively, are directed inward. Both forces consist of a chemical gradient of the ions (ΔpH or ΔpNa) and the membrane potential ($\Delta\Psi$) that is common to both forces. The gradients are maintained across the membrane by the action of primary pumps that use the free energy released in chemical reactions to pump H^+ and Na^+ across the membrane. The free energy stored in the electrochemical gradients of the ions across the cytoplasmic membrane is used to concentrate the substrate in the compartment to which it is transported. Thus, the symporter accumulates the substrate inside the cell, while the antiporter depletes the substrate from the cell. Secondary transporters that catalyze exchange are not coupled to (net) proton or Na^+ movement and are driven by the inward-directed substrate gradient and the outward-directed product gradient. Both gradients are maintained by metabolism of the substrate inside the cell, which lowers the internal substrate concentration and increases the internal product concentration. A small group of exchangers that is of particular importance to the transporter family that is the topic of this review use the free energy in the substrate and product gradients to generate metabolic energy in the form of a membrane potential. They are part of metabolic pathways that function as indirect proton pumps.

Secondary transporters are typical integral membrane proteins that fold as a bundle of hydrophobic α-helices, which are oriented more or less perpendicular to the membrane. At the two sides of the membrane, the transmembrane segments (TMSs) are connected by hydrophilic loops of various lengths. Thus far, eight three-dimensional crystal structures of secondary transporters have been described. These structures have provided a first glimpse of the structural and mechanistic diversity that may be present in the many different families of secondary transporters. The structures of the drug transporter AcrB, the lactose transporter LacY, the glycerol-P/P_i exchanger GlpT, the Na^+/H^+ antiporter NhaA, and the Cl^-/H^+ antiporter ClC, all from *Escherichia coli*; of the glutamate transporter homolog Glt_{Ph} from the archaeon *Pyrococcus horikoshii*; of the leucine transporter LeuT from *Aquifex aeolicus*; and of the mitochondrial ATP/ADP antiporter (2, 37, 47, 49, 98, 105, 153, 154) represent seven different structures and possibly as many different mechanisms (137).

Here we review the current knowledge about the 2-hydroxycarboxylate transporter (2HCT) family, a family of secondary transporters. The members are found exclusively in bacteria, and all transport substrates such as citrate, malate, and lactate. Well-studied members of the 2HCT family are the Na^+-citrate symporter CitS of *Klebsiella pneumoniae*, the malate/lactate exchanger MleP and the citrate/lactate exchanger CitP found in lactic acid bacteria, and the citrate/malate H^+-symporter CimH of *Bacillus subtilis*. The transport properties of the characterized 2HCT members will be discussed in the context of their physiological function. Based on sequence analysis and the genetic organization of the structural genes in the genomes, physiological functions are assigned to uncharacterized 2HCT members. No three-dimensional (3D) structure of any of the members of the 2HCT family is available, but a wealth of data obtained from experimental studies and computational analysis will be discussed, giving us models for the structures and translocation mechanisms of the transporters in this family.

FUNCTION

Distribution and Phylogeny

A BLAST search (4) of the NCBI nonredundant protein database, using CitS of *K. pneumoniae* as a query, yielded 37 unique sequences in the 2-hydroxycarboxylate transporter family (January 2005) (Table 1). No new sequences were detected when the original 37 were resubmitted. All members of the family are found exclusively in the bacterial kingdom. The highest frequency of 2HCT family members is observed in the phylum *Firmicutes*, the low-CG gram-positive bacteria, almost all in the class *Bacillales* with the remaining in the classes *Clostridia* and *Mollicutes*. A somewhat smaller group of transporters is found in the phylum *Proteobacteria* but exclusively in the beta and gamma subdivisions. Additionally, family members are found in the *Fusobacteria* and *Spirochaetales* phyla. The specific distribution of the transporters over the phylogenetic tree suggests that the genes were exchanged between the different bacteria late in evolution. This is supported by the facts that the genes are localized on endogenous plasmids in *Lactococcus* and *Leuconostoc* species (24, 130, 149) and that exact copies (100% sequence identity) for CitP in *Leuconostoc mesenteroides* and *Leuconostoc lactis*; for MAEN in the *Bacillus thuringiensis*, *Bacillus cereus*, and *Bacillus anthracis*; and for MalP (also termed MaeP) in *Streptococcus bovis* and *Enterococcus feacalis* are observed.

Pairwise sequence identities between the 2HCT family members ranged between 18% (ZP002741 of *Ralstonia metallidurans* and CitS_1 of *Onion yellows phytoplasma*) and 100% (see above). A subgroup of 18 sequences shared a maximal pairwise sequence identity of 60% with any other sequence in

TABLE 1. Distribution of the 2-hydroxycarboxylate family in the bacterial kingdom

Phylum and class	Organism	Genome availability[a]	2HCT[b]	Identification no.[c]	Function	Gene organization[d]
Firmicutes						
Bacillales	*Bacillus subtilis*	x	CimHbsub	16080928	H^+/malate symport H^+/citrate symport	T
	Bacillus licheniformis	x	• CimHblic	52082436		T
	Bacillus subtilis	x	MaeNbsub	16080210	Na^+/malate symport	malSR-4-T
	Bacillus licheniformis	x	• MaeNblic	52081654		malSR-5-T
	Bacillus anthracis	x	• BA1158bant	21398533		malSR-T-M
	Bacillus cereus	x	• NP830396bcer	30018765		malSR-T-M
	Bacillus thuringiensis	x	• MaeNbthu	49480168		malSR-T-M
	Bacillus clausii	x	MaeNbcla	56962691		malSR-T-M
	Bacillus halodurans	x	BH0400bhal	15612963		malSR-M-T
	Oceanobacillus iheyensis	x	• NP694139oihe	23100672		malSR-M-T
Lactobacillales	*Streptococcus bovis*		MalPsbov	1146122	H^+/malate symport	T-M
	Streptococcus pyogenes	x	• MalPspyo	15675091		malSR<>T-M
	Streptococcus agalactiae	x	• NP688909saga	22538058		malSR<>T-M
	Enterococcus faecalis	x	• NP814935efae	29375781		malSR<>T-M
	Lactococcus lactis	x	MlePllac	15672883	Malate/lactate exchange	mleR M-T
	Leuconostoc mesenteroides		• LMES0009lmes	23023296		mleR<>M-T
	Enterococcus faecium		ZP000379enfa	46189298		mleR M-T
	Leuconostoc mesenteroides		CitPlmes	623057	Citrate/lactate exchange	M-CDEFXG-R-T
	Leuconostoc lactis		• CitPlela	1079560		
	Weissella paramesenteroides		• T46734wpar	11279004		M-CDEFXG-R-T
	Lactococcus lactis	x	• CitPllac	15617471	Citrate/lactate exchange	R-T
Clostridia	*Clostridium perfringens*	x	CitNcper	18310134		R-GCDEFX-M-T
Mollicutes	*Onion yellows*	x	CitSp$on	39939206		M-T
	Onion yellows	x	CitS_1p$on	39938772		T
Proteobacteria						
Beta subdivision	*Chromobacterium violaceum*	x	MaeNcvio	34497622		T
	Burkholderia cepacia		• ZP002145bcep	46313985		
	Ralstonia metallidurans		ZP002741rmet	48769815		
	Burkholderia cepacia		• ZP002185bcep	46317973		
Gamma subdivision	*Klebsiella pneumoniae*		CitWkpne	18140906	Citrate/acetate exchange	T-X
	Erwinia carotovora	x	• CitWecar	50121500		GXFEDC-T<>AB
	Erwinia carotovora	x	MaeNecar	50123313		T><2-malSR
	Klebsiella pneumoniae		CitSkpne	399257	Na^+/citrate symport	G FEDC<>T-GAB-AB
	Salmonella enterica	x	• CitCsaen	16759051	Na^+/citrate symport	GXFEDC<>T-GAB-AB
	Photobacterium profundum	x	• YP130484ppro	54309464		GXFEDC<>T-GAB-AB[e]
	Vibrio cholerae	x	• VC0795vcho	15640813		GXFEDC<>T-GAB-AB
Fusobacteria	*Fusobacterium nucleatum*	x	FN1375fnuc	19704710		T-oadA-GDEF
Spirochaetales	*Treponema denticola*	x	NP973298tden	42528200		T

[a] "x" indicates that the complete genome sequence of the organism is available at http://www.ncbi.nlm.nih.gov/genomes/MICROBES/Complete.html.

[b] Sequences were extracted from the NCBI protein database by BLAST searches (http://www.ncbi.nlm.nih.gov/). All unique 2HCT sequences are reported. 2HCT sequences preceded by a dot are more then 60% identical to the previous sequence (typical) in the list.

[c] Unique identifier of the entry in the protein database.

[d] Abbreviations: T, transporter; M, malic enzyme; malSR, two-component signal transduction system; mleR, transcriptional regulator; R, regulatory protein CitR; GXFEDC, citrate lyase subunits and accessory proteins (see Fig. 3C); AB, two-component signal transduction system CitAB; GAB, oxaloacetate decarboxylase subunits *oadGAB* (see Fig. 3B); *oadA*, α subunit of oxaloacetate decarboxylase. Numbers indicate intergenic open reading frames. Adjacent genes are connected by a dash, adjacent but divergently transcribed genes by angle brackets, and distant genes by a space.

[e] *oadG* and *citD* were erroneously annotated in the database.

this group (typical sequences), indicating that 19 sequences in the family are very similar to one of the typical sequences (Table 1). The 2HCT family members with very similar sequences (>60% sequence identities) are in the same bacterial class and often in the same genus. However, the phylogenetic correlation between organism and amino acid sequence breaks down for more distantly related members of the family. A phylogenetic tree of the 18 typical sequences (<60% sequence identity) (Table 1) shows six clusters of sequences (Fig. 1). Except for cluster VI, which contains two sequences found in

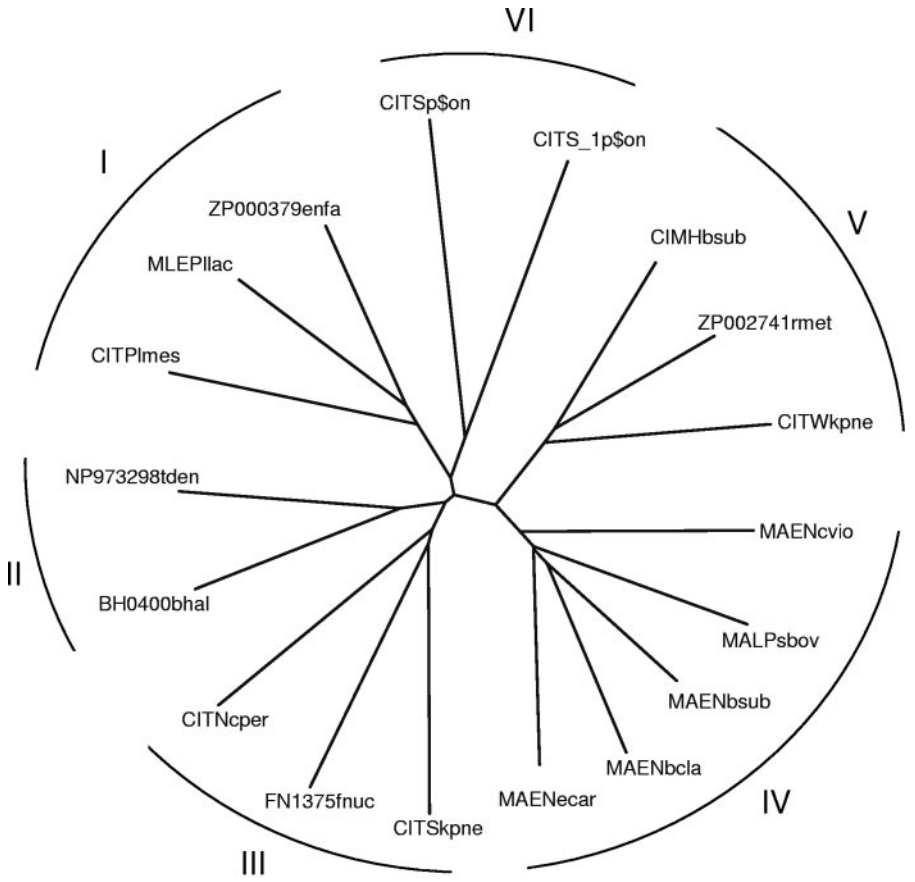

FIG. 1. Unrooted phylogenetic tree of members of the 2HCT family. Phylogenetic relationships were analyzed with the CLUSTAL W program using the default settings (141). The tree was generated with the DRAWTREE program in the Phylip package (J. Felsenstein, PHYLIP (Phylogeny Inference Package), version 3.6.a3, Department of Genome Sciences, University of Washington, Seattle, 2002). The tree is based on the C-terminal part of the multiple-sequence alignment, which contains the fewest gaps (positions 300 to 500 in Fig. 5A). Sequences included in the alignment correspond to the "typical" sequences in the "2HCT" column of Table 1. All other members of the 2HCT transporter family share over 60% sequence identity with one of the "typical" sequences. The six clusters in the tree are indicated by I to VI.

the genome of the plant pathogen *Onion yellows phytoplasma*, and cluster I, whose members belong to the same bacterial class, the clusters contain members from different phyla. Three bacteria, *B subtilis*, *K. pneumoniae*, and *Burkholderia cepacia*, contain two 2HCT family members in their genomes, which, however, are in different clusters. It follows that, for example, CIMH of *B. subtilis* (cluster V) in the phylum *Firmicutes* is more closely related to CITW in the phylum *Proteobacteria* than to MAEN (cluster IV), which is located on the same genome. It is likely that the two genes on one genome were acquired by the organism in two independent events during evolution.

Transport Properties

Seven different transporters in the 2HCT family have been functionally characterized in detail. All of them recognize either citrate, malate, or both as substrates. A common feature of the substrates is the presence of a 2-hydroxycarboxylate motif, $HO\text{-}CR_2\text{-}COO^-$ (hence the name 2HCT family, for *2-h*ydroxy*c*arboxylate *t*ransporter family). Symport was found to be the mode of energy coupling catalyzed by these transporters. However, some transporters in the family were clearly optimized to catalyze exchange between an internal and an external substrate (Table 1). Characterized Na^+ symporters in the family are the citrate transporter CitS of *K. pneumoniae* and the malate transporter MaeN of *B. subtilis* (29, 143, 151). The citrate/malate transporter CimH of *B. subtilis* and the malate transporter MalP of *S. bovis* were shown to be H^+ symporters (60, 63). The group of exchangers includes the citrate/lactate exchanger CitP of *Leuconostoc mesenteroides*, the malate/lactate exchanger MleP of *L. lactis*, and the citrate/acetate exchanger CitW of *K. pneumoniae* (58, 94, 107). The symporters in the family usually transport only one or two 2-hydroxycarboxylate substrates, while the exchangers transport a range of 2-hydroxycarboxylates (7, 50, 60, 151). The much broader substrate specificity is an inherent property of the exchangers (see below). Substrate and co-ion specificities do not correlate with the clustering of the transporters in the family tree (Fig. 1). The citrate transporters are found in clusters I, III, and V, and the malate transporters are found in clusters I, IV, and V. The Na^+ symporters are found in clusters III and IV, the H^+ symporters are in clusters IV and V, and the exchangers are in clusters I and V. Apparently, substrate and

co-ion specificity are details in the primary structure and, most likely, in the 3D structure of the proteins as well.

The citrate transporter CitS of *K. pneumoniae* is by far the best-studied transporter in the 2HCT family. Nevertheless, the exact stoichiometry between substrate and co-ions has still not been resolved. Dimroth and Thomer (30) reported that citrate transport catalyzed by CitS was Na^+ dependent and proposed that translocation involved symport of trivalent citrate (cit^{3-}) with three Na^+ ions (30). The proposal was based on the observed lack of charge translocation during turnover (electroneutral transport), which, however, was disputed in other studies (142, 143). Moreover, the latter studies reported that the proton gradient across the membrane was a driving force, suggesting that in addition to Na^+ ions, protons were cotransported. Since at physiological conditions, the divalent form of citrate is most abundant, it was proposed that $Hcit^{2-}$ would be symported with at least three co-ions, including both Na^+ and H^+ (142, 143). The affinity of the transporter for total citrate was found to be about 10 μM at a pH range of between 5.5 and 6.5. Kinetic analysis of citrate uptake measured in *E. coli* cells expressing CitS revealed that translocation of citrate is coupled to translocation of two sodium ions (76), a result that was confirmed much later by uptake studies in right-side-out membrane vesicles (134). The relationship between the uptake rate and Na^+ ion concentration was shown to be sigmoid, with approximately 3 mM Na^+ yielding half of the maximal rate. The coupling stoichiometry of two Na^+ ions was observed at the pH range of pH 6 to 8, suggesting that H^+ does not compete with Na^+ for the two binding sites (76). A strict coupling between citrate and Na^+ ions is also supported by point mutations that lower the affinity for Na^+ by an order of magnitude but leave the stoichiometry unaltered (135). The differing opinions on the coupling stoichiometry of CitS extend to the kinetic mechanism of the transporter (see "Kinetics" in "MECHANISMS" below) (109). Little is known about the stoichiometries of the other Na^+ symporter, MaeN of *B. subtilis*, and of the H^+ symporters, MalP of *S. bovis*, and CimH of *B. subtilis* (60, 63, 151). The latter transporter is believed to catalyze electroneutral transport (63).

The exchangers in the 2HCT family belong to a special group of secondary transporters that are involved in the generation of secondary metabolic energy (78). They are precursor/product exchangers that couple the uptake of the substrate (the precursor) to the excretion of the end product of a metabolic pathway (5, 78, 107). Membrane potential is generated during turnover, because of a charge difference between the two substrates. CitP of *Leuconostoc mesenteroides* and MleP of *L. lactis* exchange internal monovalent lactate (lac^-) for external divalent citrate and malate ($Hcit^{2-}$ and mal^{2-}, respectively), which results in a membrane potential of physiological polarity (positive outside). CitP was shown to be a proton symporter with affinity for both citrate and lactate. In the symport reaction, CitP couples the translocation of $Hcit^{2-}$ to a single H^+, resulting in the translocation of one unit of negative charge per turnover. As a consequence, the symport reaction is driven by a pH gradient but is counteracted by the membrane potential (94). With lactate as the substrate, CitP catalyzes electroneutral symport of lac^- and H^+. In the exchange mode, the proton is believed to go back and forth during transport. The precursor/product exchangers are symporters that were optimized to catalyze exchange, which is their physiological function; exchange is much faster than symport (see also "Kinetics" in "MECHANISMS" below) (7, 94, 96, 107). Exchangers such as CitP and MleP recognize structurally related compounds; citrate and lactate, and malate and lactate, are pairs of 2-hydroxycarboxylates, $HO\text{-}CR_2\text{-}COO^-$, that differ in the R groups. The proteins are very specific towards the hydroxyl and carboxylate groups and, at the same time, very tolerant towards the two R groups of the molecules. As a consequence, both CitP and MleP were shown to translocate a wide range of nonphysiological substrates that differ in the R groups (7). The only restriction seems to be the size of the R group, which at the upper limit is set by the size of the physiological substrates. Thus, CitP accepts citrate, while the most bulky substrate for MleP is malate. At the lower limit, glycolate, $HO\text{-}CH_2\text{-}COO^-$ is recognized and translocated by both transporters. Nonphysiological substrates with different R groups that were shown to be translocated include the dicarboxylates tartarate, citramalate, and 2-hydroxyglutarate and the monocarboxylates mandalate, 2-hydroxyisovalerate, 2-hydroxyisobutyrate, and glycolate (7, 9). Despite the broad specificity, both CitP and MleP were found to be highly stereoselective with a strong preference for the *S* over the *R* enantiomers. The stereoselectivity was observed only with dicarboxylate substrates, suggesting a specific interaction of the protein with a carboxylate of the R group in the *S* enantiomers (9). In agreement, the affinity of both MleP and CitP for the *S* enantiomers of dicarboxylate substrates is 1 to 2 orders of magnitude higher than that observed for monocarboxylates and for the *R* enantiomers of dicarboxylates (see also "Structure-Function Relationship" in "MECHANISMS" below).

CitW of *K. pneumoniae* was shown to be a citrate/acetate exchanger and the first member of the 2HCT family where the physiological substrate is not a 2-hydroxycarboxylate (58). Previously, it was demonstrated that CitP and MleP of lactic acid bacteria showed some activity with the 2-oxocarboxylates glyoxylate and oxaloacetate (7, 9). CitW differs from CitP and MleP in that it does not share the broad substrate specificity of the latter two exchangers. Only a low activity was observed with L-malate. The transported species was shown to be $Hcit^{2-}$, suggesting electrogenic citrate/acetate exchange, but the electrogenicity was not demonstrated.

Physiological Function

The physiological substrates of the characterized members of the 2HCT family are citrate and malate, and it is to be expected that they function in the breakdown pathways of these two substrates. Four different pathways in which 2HCT transporters are involved have been identified, two for malate and two for citrate (Fig. 2). The pathways are mainly anaerobic breakdown routes for the two substrates and are characterized by decarboxylation steps of cytoplasmic malate or oxaloacetate. The lactic acid bacteria in the phylum *Firmicutes* are typically facultative anaerobes in which di- and tricarboxylates are degraded to lactate or pyruvate. The malate/lactate exchanger MleP of *L. lactis* functions in malolactic fermentation, a secondary metabolic energy-generating pathway in which malate is converted into lactate and carbon dioxide (Fig. 2A). Similarly, the citrate/lactate exchanger CitP of *Leuconostoc*

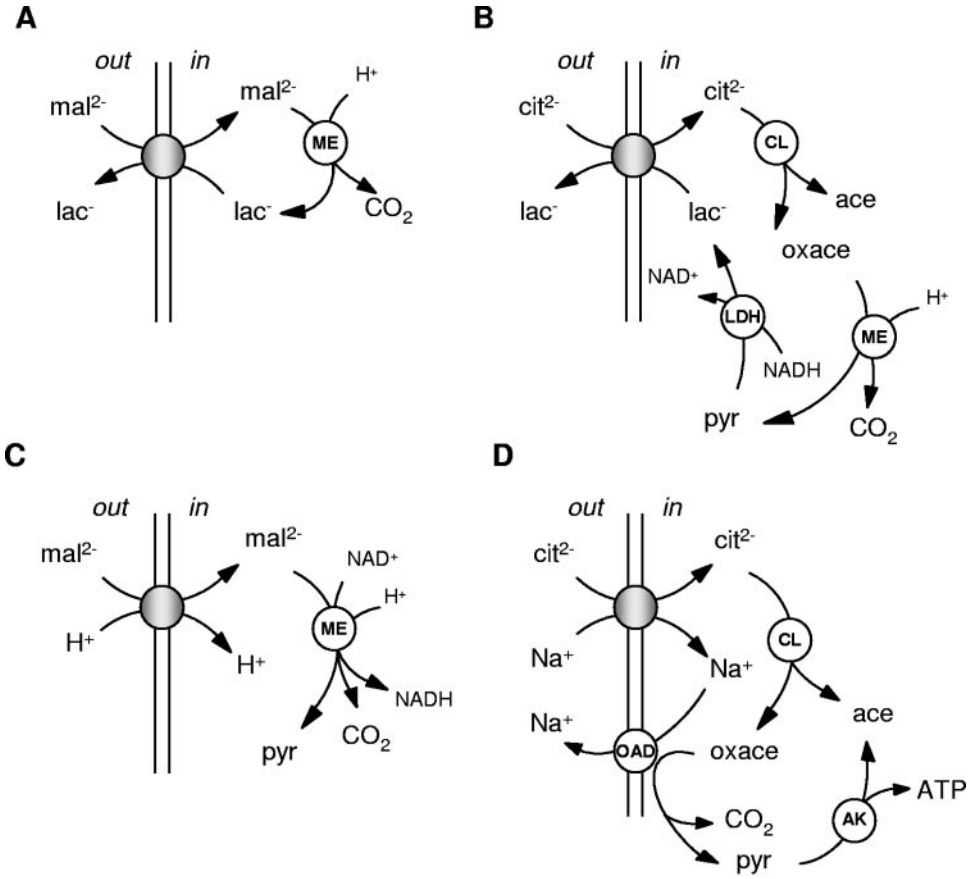

FIG. 2. Schematic representation of physiological pathways for citrate and malate degradation involving 2HCT family members. (A) Malolactic fermentation; (B) citrolactic fermentation; (C) oxidative malate decarboxylation pathway; (D) citrate fermentation in gram-negative bacteria. Shaded circles represent the 2HCT transporter proteins. The stoichiometry of the transporters and the pyruvate lyase step are omitted in panel D. Abbreviations: cit, citrate; mal, malate; lac, lactate; oxace, oxaloacetate; ace, acetate; pyr, pyruvate; ME, malic enzyme; CL, citrate lyase; OAD, oxaloacetate decarboxylase; LDH, lactate dehydrogenase; AK, acetate kinase.

mesenteroides and *L. lactis* functions in citrolactic fermentation, a more complex example of a secondary proton motive force-generating pathway which converts citrate into lactate, acetate, and carbon dioxide. Decarboxylation of oxaloacetate yielding pyruvate is a step in the pathway (Fig. 2B). The H^+/malate symporter MalP of *S. bovis* is involved in the breakdown of malate to pyruvate by oxidative decarboxylation (Fig. 2C). *B. subtilis*, in the phylum *Firmicutes*, is known to be able to grow on most of the Krebs cycle intermediates under aerobic conditions. The Na^+/malate symporter MaeN is essential for growth on malate. Oxidative decarboxylation of malate to pyruvate is likely to be part of the metabolism as well. Finally, the gamma subdivision of the *Proteobacteria* contains many bacteria that can grow under both aerobic and anaerobic conditions. While under aerobic conditions citrate is degraded in the Krebs cycle, under anaerobic conditions the Na^+/citrate transporter CitS of *K. pneumoniae* was shown to be involved in one of the fermentative pathways for citrate breakdown which results in the formation of ATP (Fig. 2D). The energetics of the pathway is quite different from that of the citrate breakdown pathway in the lactic acid bacteria but involves decarboxylation of oxaloacetate to pyruvate as well. The different pathways correlate with clusters of genes in the genomes that include those for regulatory proteins, metabolic enzymes, and transporters (Table 1). These clusters may be used to assign specific functions to uncharacterized transporters in the family.

Malolactic fermentation. The malolactic fermentation pathway consists of two enzymes, the transporter, MleP, and the malolactic enzyme, MleS. The pathway converts malate into lactate (Fig. 2A). MleP is responsible for both the uptake of malate and the excretion of the end product lactate (precursor/product exchange [78, 107]) Internalized malate is decarboxylated by MleS, a member of a large family of malic enzymes that, upon releasing carbon dioxide, convert malate into lactate (MleS), malate into pyruvate (MalS), or oxaloacetate into pyruvate (CitM). The conversion of malate to pyruvate proceeds by a stepwise mechanism (Fig. 3A) (74). Malate is first converted to oxaloacetate, followed by decarboxylation of the latter to pyruvate. The first step is coupled to the reduction of $NAD(P)^+$; the latter consumes a cytoplasmic proton. Malic enzymes that have oxaloacetate decarboxylation activity are believed to allow the substrate to enter the sequence in the second step. Malolactic enzymes (MleS) are believed to add the reduction

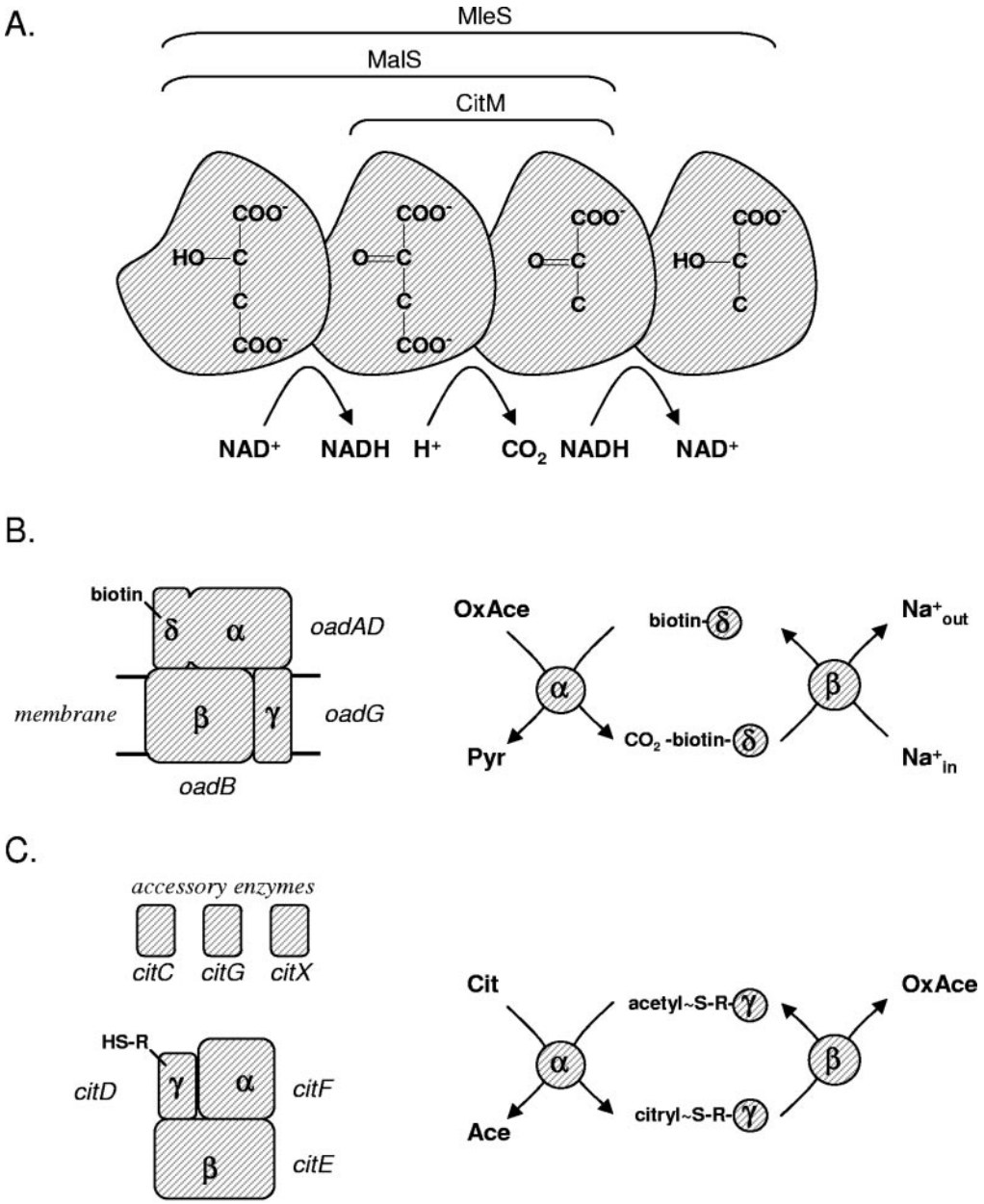

FIG. 3. Mechanism of enzymes involved in citrate and malate metabolic pathways. (A) Malic enzymes. Malic enzyme homologs catalyze the conversion of malate to oxaloacetate, oxaloacetate to pyruvate, and pyruvate to lactate, while the substrate remains bound to the enzyme. Different types of malic enzymes (MleS, MalS, and CitM) catalyze different parts of the sequence as indicated at the top. (B) Oxaloacetate decarboxylase. Left, the OAD complex of *K. pneumoniae*, showing the domain, subunit composition, and the names of the corresponding structural genes. Right, mechanism of catalysis. The α domain on the αδ subunit transfers the carboxyl group of oxaloacetate to the biotin group attached to the δ domain, after which the decarboxylation of the carboxy-biotin group is coupled to the pumping of Na^+ ions across the membrane. (C) Citrate lyase. Left, composition of the CL complex and the accessory enzymes necessary for the incorporation and activation of the modified CoA prosthetic group R-SH (2′-(5″-phosphoribosyl)-3′-dephospho-CoA) on the gamma subunit. The corresponding structural genes are indicated as well. Right, mechanism of catalysis. The gamma subunit is an intermediate acyl carrier protein that cycles between the citryl- and acetyl-loaded state during turnover. Abbreviations: Cit, citrate; OxAce, oxaloacetate; Ace, acetate; Pyr, pyruvate.

of pyruvate to lactate as a third step to the sequence (Fig. 3A). The cofactor NAD^+ is tightly bound to the enzyme and accepts the electrons in the malate dehydrogenase step. Following decarboxylation to pyruvate, the electrons are transferred back to the pyruvate molecule, which dissociates from the enzyme only upon reduction to lactate. The cofactor NAD cycles between the oxidized and reduced states during turnover, making the conversion redox neutral.

The physiological function of the malolactic fermentation pathway is the generation of proton motive force that is used as

an energy source for cellular processes. The two components of the proton motive force, the pH gradient and the membrane potential, are generated in two separate steps of the pathway by a secondary metabolic energy generation mechanism (78). Because of the difference in charge between divalent malate and monovalent lactate, the exchange activity of MleP results in a membrane potential, with positive out. The consumption of a proton in the decarboxylation of malate by MleS results in alkalinization of the cytoplasm and, consequently, in a pH gradient (77). In the steady state of malate degradation, the pathway results in alkalinization of the external medium, which could provide an additional physiological function for the pathway.

The malolactic fermentation pathway is not general to lactic acid bacteria, but is observed only in certain strains of *Lactococcus*, *Lactobacillus*, *Pediococcus*, and *Leuconostoc*. The process is best studied in *Oenococcus oeni*, a bacterium which plays an important role in the nonalcoholic fermentation in wine production (73, 83). Conversion of malate into lactate is an important step in the deacidification of wine following the alcoholic fermentation. The pathway in *O. oeni* (previously known as *Leuconostoc oenos*) is slightly different from the one described above for *L. lactis*, and the transporter is not a member of the 2HCT family. Rather than malate^{2-}/lactate^{-} exchange, the transporter of *O. oeni* catalyzes uniport of monovalent malate (Hmal^{-}) (120). The effect on the membrane potential is the same: net negative charge is moved into the cell. Inside the cell, malolactic enzyme converts Hmal^{-} into lactic acid (Hlac), thereby consuming a proton and releasing carbon dioxide. Lactic acid leaves the cell by passive diffusion. The energetic consequences of the pathway are the same, but the pathway is better adapted to the acidic conditions of wine fermentation (119). The transporter that catalyzes the electrogenic uniport reaction is a member of the auxin efflux carrier (AEC) family (TC 2.A.69 in the transporter classification system [17, 117]), which contains many members from bacteria, archaea, and plants (70).

Decarboxylation pathways built from a precursor/product exchanger and a decarboxylase are not restricted to lactic acid bacteria or to malate as the substrate. One of the first pathways described was the decarboxylation of oxalate to formate in *Oxalobacter formigenes*. The conversion is the main energy source for ATP production in this obligate anaerobic bacterium (5). Electrogenic exchange between divalent oxalate and monovalent formate is catalyzed by OxlT, a transporter from the major facilitator superfamily (MFS) (TC 2.A.1) (1). Another group of decarboxylation pathways is formed by the decarboxylation of amino acids, yielding biogenic amines. Examples are histidine to histamine and tyrosine to tyramine (20, 86, 87, 97). The exchangers that couple the uptake of the amino acid to the excretion of the amine are members of the amino acid-polyamine-choline superfamily (TC 2.A.3). Apparently, nature has implemented analogous pathways by selecting the appropriate transporters, and also decarboxylases, from different gene families.

Genetic organization of malolactic fermentation genes. In *L. lactis*, the genes coding for the decarboxylase MleS and the transporter MleP are organized in an operon structure in the order *mleS-mleP* (M-T) (Table 1). Upstream of *mleS*, but separated by 27 other genes, the *mleR* gene codes for a positive regulator of expression of the malolactic operon that senses the presence of L-malate. MleR is a member of the LysR family of activators (114). The three proteins MleR, MleS, and MleP are characteristic of the malolactic fermentation pathway, and highly similar proteins are encoded in the genome of *Leuconostoc mesenteroides* (6, 26). Here, the *mleR* gene is found immediately upstream of the *mleS-mleP* pair but divergently transcribed. The operon organization in which the malic enzyme is followed by the transporter is also found in the genome of *Enterococcus faecium.* Moreover, the transporter, ZP000379, clusters with MleP of *L. lactis* and *Leuconostoc mesenteroides* on the phylogenetic tree of the transporters (Fig. 1, cluster I), strongly suggesting that the two genes code for a malolactic fermentation pathway. Similarly to the case for *L. lactis*, a homologous gene coding for the transcriptional regulator MleR is located distantly on the chromosome. The two transporters of the plant pathogen *Onion yellows phytoplasma* in cluster VI of the phylogenetic tree (Fig. 1) are loosely associated with the transporters in cluster I, and the gene coding for CitSp$on is preceded by a malic enzyme homolog (Table 1). However, the latter is quite distant from the malolactic enzymes associated with the transporters in cluster I, and since no *mleR* homolog is found in the genome, the two genes are not likely to form a malolactic operon.

The genetic organization of the malolactic operon in the wine bacterium *O. oeni* is identical to that observed in *Leuconostoc mesenteroides*; a divergently transcribed regulator gene precedes the malic enzyme/transporter pair (R<>M-T) (69). Strikingly, however, as mentioned above, the transporter MleP of *O. oeni* is a member of the AEC rather than the 2HCT transporter family. In fact, a search of 156 completed bacterial genomes available at the microbial genome site of the NCBI (http://www.ncbi.nlm.nih.gov/genomes/MICROBES/Complete.html; April 2005) for the combination of the three genes characteristic of malolactic fermentation, *mleR*, *mleS*, and *mleP*, showed that transporters of the AEC family are most frequently observed in conjunction with MleS (Table 2). The search showed that the malolactic fermentation pathway is quite rare in the bacterial kingdom and is only found in low-GC gram-positive organisms. However, even then, the capacity is not at all general, with only 5 out of 38 genomes from the phylum *Firmicutes* coding for the pathway (Table 2). In this group, the malic enzymes and transcriptional regulators represent highly conserved groups of proteins, with >50 and >30% sequence identity for MleS and MleR, respectively. In contrast, the divergence in the associated transporters is remarkable. *Lactobacillus plantarum*, *Lactobacillus acidophilus*, and *Streptococcus mutants* use a transporter of the AEC family for the uptake of malate, as was described for *O. oeni* above. *L. lactis* uses a transporter of the 2HCT family, and *Clostridium acetobutylicum* uses one of the [st303]AIT family. Members of the latter family are known to catalyze exchange; e.g., CitT of *E. coli* catalyzes citrate/succinate exchange, and SODiT1 of spinach chloroplasts catalyzes 2-oxoglutarate/malate exchange (110). It is likely that the transporter of *C. acetobutylicum* catalyzes malate/lactate exchange, as does MleP of *L. lactis*. Both the [st326]2HCT and [st303]AIT1 transporter families are found in structural class ST[3] in the MemGen classification (see "Primary Structure" in "STRUCTURE" below) and may well be distantly related.

Oxidative malate decarboxylation pathway. In the rumen bacterium *S. bovis*, uptake of malate by MalP of the 2HCT

TABLE 2. Distribution of (putative) malolactic fermentation over 156 sequenced bacterial genomes (207 strains)

Phylum and class	n[a]	Bacterium	Transporter family	Gene clustering[b]
Actinobacteria	15			
Aquificae	1			
Bacteroidetes	3			
Chlamydales	6			
Chlorobi	1			
Chloroflexi	1			
Cyanobacteria	7			
Deinococcus	2			
Firmicutes	38			
Bacillales	23	*Lactococcus lactis*	[st326]2HCT	mleR-27-M-T
		Lactobacillus plantarum	2.A.69 AEC	mleR<>M-T
		Lactobacillus acidophilus	2.A.69 AEC	T mleR<>M
		Streptococcus mutans	2.A.69 AEC	mleR-1<>M-T
Clostridia	4	*Clostridium acetobutylicum*	[st303]AIT1	T-M-mleR
Fusobacteria	1			
Planctomycetes	1			
Proteobacteria	74			
Spirochaetales	5			
Thermotogae	1			

[a] Number of completed genomes available at http://www.ncbi.nlm.nih.gov/genomes/MICROBES/Complete.html.
[b] Abbreviations: T, transporter MleP; M, malic enzyme MleS; mleR, transcriptional regulator; Numbers indicate intergenic open reading frames. Adjacent genes are connected by a dash and adjacent but divergently transcribed genes by angle brackets.

family is coupled to an oxidative-type malic enzyme (MalS) that converts malate to pyruvate and carbon dioxide and NAD^+ to NADH (Fig. 2C and 3A) (59, 60). Malate is transported into the cell in symport with protons, an energy-requiring process. The advantage for the cell must, therefore, lie in the production of redox equivalents in the form of NADH or in the production of pyruvate, which is a central metabolite. The different physiological function of the pathway correlates with a different operon structure, where the gene coding for the malic enzyme is downstream of the gene for the transporter (T-M) (Table 1) (59). The same organization is found on the chromosome for the close homologs of MalP in *Streptococcus pyogenes*, *Streptococcus agalactiae*, and *E. faecalis* (Fig. 1, cluster IV). The genome sequences of these three organisms show that two genes coding for a two-component signal transduction system are divergently transcribed relative to the T-M pair (malSR) (Table 1) and are located immediately upstream of the transporter gene *malP*. The response regulator and sensor kinase encoded by the two genes are close homologs of the corresponding proteins of two-component systems specific for di- and tricarboxylates, such as the C_4-dicarboxylate-sensing DcuSR system of *E. coli* and the citrate-sensing CitAB system of *K. pneumoniae* (41, 54). It is to be expected that the two-component system is also present in the genome of *S. bovis* and that the gene cluster malSR<>T-M is responsible for the sensing of L-malate in the medium and, subsequently, the uptake into the cell and breakdown to pyruvate.

In *B. subtilis*, the Na^+/malate symporter MaeN, which is closely related to the H^+/malate symporter of *S. bovis* (Fig. 1, cluster IV), is essential for the uptake of malate from the medium during growth on malate as the sole carbon source. A transcriptome analysis showed that the transporter is induced by the presence of malate in the medium, which is mediated by a two-component signal transduction system, YufLM (140). The two-component system is similar to the MalSR system in *S. bovis* and is encoded upstream of the transporter gene, separated by four other genes (Table 1). The same organization is observed in the genome of *Bacillus licheniformis*. Transcriptional analysis revealed coinduction via the two-component system of YwkA, one of four malic enzyme homologs encoded in the genome of *B. subtilis*. YwkA was shown to be a malic enzyme of the oxidative malate decarboxylation type, strongly suggesting that the malate-to-pyruvate pathway is operative in *B. subtilis* (33). It should be noted that while the transporter MaeN was shown to be essential for growth on malate, the *ywkA* gene product was not. Instead, a constitutively expressed malic enzyme homolog of the oxidative type, encoded by the *ytsJ* gene, was essential (33). Moreover, the *ywkA* gene is transcribed in a single transcript with *ywkB*, coding for an AEC family transporter, which may encode a malate transporter as well (see previous section). Other transporters that are likely to play a role in malate metabolism in *B. subtilis* are YflS in the [st303]AIT family, a transporter which is also part of the YufLM regulon, and CimH in cluster V of the 2HCT family (Fig. 1). The presence of the gene coding for CimH correlates with the presence of the malSR-4/5-MaeN gene cluster in the genomes of *B. subtilis* and *B. licheniformis* (Table 1). CimH of *B. subtilis* transports citrate with a high affinity but a low maximal rate and transports malate with a low affinity but a high maximal rate (63). It has been suggested that CimH and MaeN would cover efficient uptake over a large range of malate concentrations in the medium (66). MaeN would take care of the lower concentrations and CimH of the higher concentrations. Unfortunately, no conditions under which the CimH protein is expressed have been identified (66, 140). The interplay between the different malate transporters and decarboxylases in *B. subtilis* needs to be investigated further.

The 2HCT members from several *Bacillus* species found in phylogenetic clusters II and IV (Fig. 1) are organized in gene clusters together with a malic enzyme homolog and a MalSR two-component signal transduction system, suggesting their involvement in oxidative malate decarboxylation pathways

(Table 1). In contrast to the clusters in the genomes of the lactic acid bacteria, the genes coding for the two-component systems of *Bacillus anthracis*, *Bacillus cereus*, *Bacillus thuringiensis*, and *Bacillus clausii* (cluster IV) are transcribed in the same direction (malSR-T-M), while in *Bacillus halodurans* (139) and *Oceanobacillus iheyensis* (cluster II) the order of the transporter and malic enzyme is reversed. MaeN of *Erwinia carotovora* in cluster IV is the only transporter in the gamma subdivision of the phylum *Proteobacteria* which is clustered with a MalSR two-component system. As in *B. subtilis* and *B. licheniformis*, a malic enzyme homolog is missing and is probably located elsewhere in the genome. The remaining transporters in clusters II and IV, MaeN of *Chromobacterium violaceum* from the beta subdivision of the *Proteobacteria* and NP973298 of *Treponema denticola* from the phylum *Spirochaetales*, are associated neither with a malic enzyme nor with a two-component signal transduction system. The gene coding for MaeN of *C. violaceum* is clustered together with the genes for the two subunits of 3-isopropylmalate dehydratase, an enzyme in the leucine biosynthetic pathway. Possibly, the transporter is involved in the uptake of the intermediate 3-isopropylmalate rather than malate.

Citrolactic fermentation. Lactic acid bacteria in the phylum *Firmicutes* are facultative anaerobic bacteria that cannot grow on citrate as the sole source of carbon and energy, but many species are known to ferment citrate in cometabolism with a carbohydrate. The citrolactic fermentation pathway, like the malolactic fermentation pathway, is a secondary metabolic energy-generating route that produces proton motive force (96). The transporter involved in the uptake of citrate from the medium is the citrate/lactate exchanger, CitP, of the 2HCT transporter family. Exchange of divalent citrate for monovalent lactate by CitP yields a membrane potential of physiological polarity. Inside the cell, citrate is split by citrate lyase (CL), yielding oxaloacetate and acetate (Fig. 2B). The latter leaves the cell by passive diffusion. A cytoplasmic enzyme, oxaloacetate decarboxylase (CitM), converts oxaloacetate into pyruvate and carbon dioxide. This is the step in which a pH gradient is generated as the decarboxylation reaction consumes a cytoplasmic proton (77, 78). Therefore, like for malolactic fermentation, the proton motive force-generating system is built around a precursor/product exchanger (CitP) and a decarboxylase (CitM). The latter was recently shown to be a member of the malic enzyme family, to which malolactic enzyme (MleS) and the oxidative malate decarboxylase (MalS) also belong (129). The oxaloacetate decarboxylases are closely related to the MalS type of malic enzymes, which decarboxylate malate to pyruvate. Mechanistically, the conversion of malate to pyruvate by MalS proceeds via oxaloacetate (Fig. 3A). The electrons are donated to the cofactor $NAD(P)^+$, while the subsequent decarboxylation of oxaloacetate to pyruvate is redox neutral. CitM is believed to skip the first step and to accept oxaloacetate directly as the substrate. NAD^+/NADH was shown to be nonessential to the oxaloacetate decarboxylation activity. Nevertheless, the cofactor binding site appears to be conserved in the CitM proteins, and the ability to bind NAD^+ and NADH was demonstrated by inhibition of enzyme activity in their presence (129).

The common decarboxylation step catalyzed by enzymes from the same family and the 50% sequence identity shared by the exchangers CitP and MleP (7) in cluster I on the phylogenetic tree (Fig. 1) indicate that the citrolactic and malolactic fermentation pathways are evolutionarily related. In *Leuconostoc mesenteroides* and *Weissella paramesenteroides*, all the genes involved in the citrolactic fermentation pathway are organized in a single operon that is located on a 22-kb plasmid. A transcriptional regulator (*citR*) and the citrate/lactate exchanger (*citP*) are downstream of the *citDEFXG* genes, coding for the citrate lyase subunits and accessory proteins, while the oxaloacetate decarboxylase gene (*citM*) is upstream (Table 1) (12, 13, 91). In *L. lactis*, the pathway is encoded in two separate operons; the transcriptional regulator is encoded together with the transporter on an 8-kb plasmid, while the remaining metabolic enzymes are encoded on the chromosome (35, 84, 88, 149). The only 2HCT transporter found in a *Clostridium* species, CitN in *Clostridium perfringens*, is also clustered with the citrate lyase genes and a malic enzyme homolog, suggesting its involvement in citrate degradation (Table 1). The order of the genes differs from the one in the lactobacilli; the malic enzyme is in between the citrate lyase genes and the transporter, while the *citR* and *citG* genes are upstream. CitN is closely related to the citrate transporters found in the gamma subdivision of the *Proteobacteria* (Fig. 1, cluster III).

The link between citrolactic fermentation and carbohydrate metabolism is evident, since lactate is a product of carbohydrate metabolism rather than citrate degradation. The pathways for citrate breakdown and carbohydrate breakdown merge at pyruvate, which subsequently, is reduced by lactate dehydrogenase to yield lactate, the substrate of the exchanger CitP (Fig. 2B). The redox equivalents necessary for the reduction are produced in glycolysis. Therefore, citrate fermentation is dependent on glycolysis. The coupling between the two pathways and the effect of citrate on growth are different for homofermentative and heterofermentative species (8, 48, 121). Homofermentative *Lactococcus* species produce 2 moles of pyruvate and, subsequently, of lactate per mole of glucose. The 2 moles of NADH needed for the reduction of pyruvate are produced in the earlier steps of the glycolytic pathway, which makes the pathway redox neutral as a whole. The end product, lactate, is used by CitP to take up citrate from the medium. The surplus of pyruvate fed into the pyruvate pool by citrate degradation is converted in a redox-neutral manner into aroma compounds such as diacetyl, a typical product of citrate/carbohydrate cometabolism. Heterofermentative *Leuconostoc* species yield 1 mol of ATP per mole of glucose, producing 1 mol of pyruvate and 1 mol of acetylphosphate (acetyl-P), which are reduced to 1 mol of lactate and 1 mol of ethanol, respectively, to balance the redox equivalents produced upstream in glycolysis. The more advantageous conversion of acetyl-P to acetate by acetate kinase, which would yield one more mole of ATP, would result in detrimental accumulation of redox equivalents and inhibition of growth. Consequently, the yield of ATP per mole of glucose is only 1 for a heterofermentative bacterium and 2 for a homofermentative bacterium. However, in the presence of citrate, pyruvate produced from citrate provides an alternative redox sink, allowing the conversion of acetyl-P to acetate. Citrate induces a metabolic shift from ethanol to acetate production with concomitant formation of additional ATP. The yield increases from 1 to 2 mol of ATP per mole of

glucose. In *Leuconostoc mesenteroides*, lactate excreted by CitP is a more direct product of citrate fermentation, needing only the redox equivalents from glycolysis (89).

The proton motive force generated in the citrate degradation pathway is in addition to the proton gradient generated by F_0F_1-ATPase at the expense of ATP produced by substrate-level phosphorylation in glycolysis. Since the hydrolysis of one ATP is coupled to the pumping of three or four H^+ ions across the membrane, the relative contribution of the metabolic energy generated by the secondary mechanism in the citrate degradation pathway is likely to be small when the fluxes through the two pathways are coupled. Assuming that energy is growth rate limiting, this is supported by the similar growth rates observed for *L. lactis* on glucose and on glucose/citrate (18, 138). In *Leuconostoc mesenteroides*, the energetic consequence of citrate cometabolism is more pronounced, but mainly because the ATP yield of glycolysis increases when metabolism shifts from ethanol to acetate production. Accordingly, a significant increase of growth rate is observed in the presence of citrate (19, 121, 123).

The lack of effect on the growth of *L. lactis* raises the question of the physiological benefit of the pathway in this organism. The answer is provided by the different induction profiles of the citrate metabolic pathways in *Leuconostoc* and *Lactococcus* species. In *Leuconostoc mesenteroides*, the enzymes of the pathway are induced by the presence of citrate in the medium, while in *L. lactis*, the induction additionally requires a low pH in the medium, suggesting a role in acid stress (40, 85, 89, 92, 93, 95). The conversion of carbohydrate to lactic acid results in acidification of the medium, which eventually inhibits growth. Proton consumption in the decarboxylation of oxaloacetate in the citrate degradation pathway initially results in alkalinization of the cytoplasm, but in the steady state of growth, when the pH gradient has developed, the alkalinizing effect is in the medium and counteracts the acidifying effect of glycolysis. Hence, the pH of the medium is buffered and the exponential phase of growth is prolonged during glucose/citrate cometabolism. Additionally, Magni et al. (89) demonstrated that the presence of citrate in the medium protects *L. lactis* against the toxicity exerted by lactate, which is produced in high concentrations in the medium (>10 mM) at the end of growth. Since lactic acid is a weak acid, it accumulates in the cell in response to a pH gradient across the cytoplasmic membrane. Cometabolism with citrate effectively lowers the cytoplasmic concentration of lactate by the action of the citrate/lactate exchanger CitP (89).

Citrate fermentation in the gamma subdivision of *Proteobacteria*. *K. pneumoniae* is one of the best-studied organisms with respect to citrate fermentation (for a review, see reference 14). The organism is a gram-negative bacterium that under anaerobic conditions can grow on citrate as the sole carbon and energy source. Two transporters in the 2-hydroxycarboxylate transporter family are involved in the breakdown route, CitS in cluster III of the phylogenetic tree and CitW in cluster V (Fig. 1). CitS is responsible for the uptake of citrate from the medium. The first metabolic steps in the degradation of internalized citrate are the same as those observed in lactic acid bacteria, but the energetics of the pathway are different (Fig. 2D). Citrate is converted into acetate and oxaloacetate by CL, and oxaloacetate is converted to pyruvate and carbon dioxide by an oxaloacetate decarboxylase (OAD) which differs from the malic enzyme homologs (CitM) found in gram-positive bacteria. OAD is an integral membrane protein that uses the free energy released in the decarboxylation of oxaloacetate to pump Na^+ across the membrane (29, 31). The activity of OAD recycles the sodium ions that have entered the cell in the symport reaction catalyzed by CitS. OAD consists of two integral membrane subunits, β and γ (encoded by *oadB* and *oadG*), and one membrane-associated subunit, α (encoded by *oadAD*) (152). Subunit α is the actual decarboxylase and consists of two domains, α and δ. Domain δ, the biotin acceptor domain, contains a biotin prosthetic group that accepts the carboxyl moiety of oxaloacetate in a reaction catalyzed by domain α. Subsequently, decarboxylation of the carboxybiotin group is coupled to Na^+ translocation by the β subunit (Fig. 3B). The pyruvate product is converted via acetyl-P into acetate. The latter reaction is catalyzed by acetate kinase and yields ATP, which is the main product of the citrate fermentation pathway in *K. pneumoniae*. It is believed that the exchanger, CitW, provides an additional uptake mechanism for citrate by coupling the transport of citrate into the cell to the excretion of the acetate end product produced by citrate lyase and acetate kinase (58). It is not known if the exchange is energy conserving.

The citrate fermentation pathway in *K. pneumoniae* is induced under anaerobic conditions in the presence of citrate (15, 16). The genes coding for the enzymes are clustered in the genome in two operons that are transcribed in opposite directions (Table 1). The organization in the genome is typical for the pathway in the gamma subdivision of the *Proteobacteria* and is also found in the *Salmonella enterica*, *Photobacterium profundum*, and *Vibrio cholerae* genomes. The transporters in these organisms share a high degree of similarity with CitS of *K. pneumoniae* (Fig. 1, cluster III; Table 1). The gene coding for the CitS transporter is followed by the three genes coding for the three subunits of oxaloacetate decarboxylase, OadG, OadAD, and OadB (Fig. 3B), and the CitA and CitB pair, which forms a two-component signal transduction system that senses the presence of citrate in the medium. In the opposite direction and upstream of the *citS* gene are the genes for the biosynthesis of the citrate lyase complex in the same order as observed in the genomes of the lactic acid bacteria discussed above (CDEFXG). In the *K. pneumoniae* cluster, the *citX* gene is missing, but it is located distantly in the genome next to the gene coding for the citrate/acetate exchanger CitW (125). The location of *citX* correlates with the presence of *citW* in the genome. Apparently CitW is not essential to the pathway, since the genomes of *S. enterica*, *P. profundum*, and *V. cholerae* do not contain the *citW* gene. A close homolog of CitW is found in the genome of *E. carotovora* (76% sequence identity) immediately upstream of the citrate lyase gene cluster. The CitAB two-component system is divergently transcribed, but the OAD oxaloacetate decarboxylase genes are missing.

Distribution of citrate fermentation in the bacterial kingdom. The enzyme CL, which splits citrate into oxaloacetate and acetate, is typical for bacteria and is involved in all known anaerobic bacterial citrate fermentation pathways. The presence of genes involved in the biosynthesis of CL is a diagnostic tool for the presence of the anaerobic citrate degradation pathway in the bacterium. The CL complex is built from three

TABLE 3. Distribution of citrate fermentation over 156 sequenced bacterial genomes (207 strains)

Phylum and class	n[a]	Bacterium	Presence of: CitM	OAD A	OAD D	OAD B	OAD G	CitR	CitAB	Transporter family	Gene organization[b]
Firmicutes	38										
Bacillales	23	*Lactococcus lactis*	x					x		[st326]2HCT	(R-T)[c] M><R<>C-DEF-X-G
		Lactobacillus plantarum	x					x		[st303]AIT	G-4-MDH-T><R<>M-C-DEF-FU-FR-2-X
		Lactobacillus acidophilus						x		[st303]AIT	FU-FR-MDH-1-T-1-C-DEF-1><5-R X G
		Streptococcus mutans		x	x	x				[st301]CITM	C-G-1-T<>1-D-B-DEF-X-A
		Streptococcus pyogenes		x	x	x				[st301]CITM	G-1-T-1-D-B-DEF-X-A-C
		Enterococcus faecalis	x	x	x	x				[st301]CITM	T-1-D-B-1-C-DEF-X-A-M-G
Clostridia	4	*Clostridium perfringens*	x					x		[st326]2HCT	R-G-C-DEF-X-M-T
		Clostridium tetani								-	DEF-C-X-G[d]
		Clostridium tetani	x							[st313]AITC	DEF-T-1-M[d]
Fusobacteria	1	*Fusobacterium nucleatum*		x						[st326]2HCT	C-X T-A-G-DEF
Proteobacteria	74										
Gamma subdivision	34	*Photobacterium profundum*		x	x	x	x		x	[st326]2HCT	BA-B-A:D-oG-T<>C-DEF-X-G[d]
		Salmonella typhimurium		x	x	x	x		x	[st326]2HCT	BA-B-A:D-oG-T<>C-DEF-X-G
		Salmonella enterica		x	x	x	x		x	[st326]2HCT	BA-B-A:D-oG-T<>C-DEF-X-G
		Vibrio cholerae		x	x	x	x		x	[st326]2HCT	BA-B-A:D-oG-T<>C-DEF-X-G
		Escherichia coli							x	[st303]AIT	BA<>C-DEF-X-G-T
		Salmonella typhimurium							x	[st303]AIT	BA<>C-DEF-X-G-T
		Salmonella enterica							x	[st303]AIT	BA<>C-DEF-X-G-T
		Haemophilus influenza								[st303]AIT	C-DEF-X:G-T
		Haemophilus ducreyi	x							[st303]AIT	C-DEF-X:G-T-M
		Shigella flexneri								[st303]AIT	C-DEF-X-G-T[e]
		Erwinia carotovora							x	[st326]2HCT	BA<>T-1-C-DEF-X-G
Spirochaetales	5	*Treponema denticola*		x	x	x				[st326]2HCT?	A:D-B C-X:G DEF T

[a] Number of completed genomes available at http://www.ncbi.nlm.nih.gov/genomes/MICROBES/Complete.html. For the remaining completed genomes, see Table 2.
[b] abbreviations: R, transcriptional regulator CitR; T, transporter; M, malic enzyme CitM; C, DEF, X, and G, citrate lyase subunits and accessory proteins (see Fig. 3C); MDH, malate dehydrogenase; FU, fumarase; FR, fumarate reductase; D, B, and A, subunits of the oxaloacetate decarboxylase OadDBA (see Fig. 3B); oG, γ subunit of oxaloacetate decarboxylase; BA, two-component signal transduction system CitAB. Adjacent genes are connected by a dash, adjacent but divergently transcribed genes by angle brackets, and distant genes by a space. Numbers indicate intergenic open reading frames. A ":" indicates that the genes are fused in one open reading frame.
[c] Plasmidic.
[d] *oadG* and/or *citD* erroneously annotated or not annotated in the database.
[e] T not annotated in the database.

different subunits, α, β, and γ, which are encoded by the *citF*, *citE*, and *citD* genes, respectively (Fig. 3C). Subunit γ is an acyl carrier protein that carries the acetyl group via a thioester bond on a coenzyme A (CoA)-derived prosthetic group covalently linked to the protein at a serine residue. The acetyl-loaded γ subunit is an intermediate during catalysis. Subunit α replaces the acetyl group with a citryl group with the release of acetate. Subsequently, subunit β regenerates the acetyl-loaded state of the cofactor by releasing oxaloacetate from the citryl group. Three additional gene products are involved in the maturation of the CL complex. CitG is involved in the modification of the CoA cofactor, CitX in the attachment of the prosthetic group to the γ subunit, and CitC in the activation of the group by catalyzing the initial acetylation (124).

The citrate lyase genes are encoded in the genomes of only 19 of the 156 bacteria listed in Table 2 and for which the complete genome sequences are available (Table 3). Each organism listed in Table 3 contains a complete set of the three structural genes *citDEF* and the three accessory genes *citC*, *citX*, and *citG*, indicating that active CL complexes are produced. *Salmonella enterica* and *Salmonella enterica* serovar Typhimurium each contain two sets of the genes, while *Clostridium tetani* contains an extra set of the structural genes, but not of the accessory genes. The CL genes are found mainly in the *Bacillales* and *Clostridia* of the phylum *Firmicutes* and in the gamma subdivision of the *Proteobacteria*. In part this may be due to the low number of sequenced genomes of organisms from many of the other phyla. It seems safe to conclude that citrate fermentation is not a trait present in the phylum *Actinobacteria*, the *Mollicutes* in the *Firmicutes*, and the alpha and beta subdivisions of the *Proteobacteria* (see Table 2 for the number of finished genomes). In the gamma subdivision, the genes are remarkably well-conserved in the order CDEFXG. In *Haemophilus influenzae* and *Haemophilus ducreyi*, the CitX and CitG proteins are combined as two domains in a single polypeptide chain. In the *Firmicutes*, the order of the structural genes *citDEF* is also conserved, but the positions of the accessory genes are more variable (Table 3). A noteworthy difference between the pathways in *Proteobacteria* and *Firmicutes* is that in the former regulation of expression seems to involve a two-component signal transduction system (CitAB), while in the latter a transcriptional regulator, CitR, is involved.

The clusters containing the CL genes in the different bacteria seem to fall into three different types: (i) those that are associated with a malic enzyme (CitM), found mainly in the phylum *Firmicutes*; (ii) those with an oxaloacetate decarboxylase type (OAD), found in all four phyla; and (iii) those not associated with a decarboxylase, found mainly in the gamma

subdivision of the *Proteobacteria*. In addition to the transporters of the 2HCT family, transporters from three other families, [st303]AIT, [st301]CITM, and [st313]AITC, are associated with the different clusters. The transporter families are all in the same structural class, ST[3], of secondary transporters in the MemGen classification (see "Primary structure" in "STRUCTURE" below). The malic enzyme- and the OAD-containing clusters represent pathways in which citrate is initially degraded to pyruvate, as described for the CitM-dependent citrolactic fermentation pathway and the OAD-dependent pathway in *K. pneumoniae* (see previous sections). The clusters without a decarboxylase represent pathways in which citrate is converted to succinate. The pathway in *E. coli* is the prototype of the latter. In contrast to *K. pneumoniae*, *E. coli* is not able to grow on citrate under aerobic conditions, because it lacks a transporter for the uptake from the medium. This property is a diagnostic tool for the difference between the two related bacteria. Under anaerobic conditions, both can grow on citrate, but they use different fermentation pathways. While *K. pneumoniae* converts citrate into acetate by using the pathway involving OAD and the 2HCT transporter CitS discussed above, *E. coli* converts citrate into the succinate end product by reduction of oxaloacetate (14). Following the first common step, catalyzed by citrate lyase and yielding oxaloacetate, the latter is converted to malate by malate dehydrogenase, then to fumarate by fumarase, and finally to succinate by fumarate reductase. The uptake of citrate is coupled to the excretion of succinate by the CitT transporter, which is a member of the [st303]AIT family in structural class ST[3] (TC 2.A.47 DASS) (110). This transporter family was discussed above in relation to malolactic fermentation in *C. acetobutylicum*.

The CL gene clusters lacking an oxaloacetate decarboxylase gene are found mainly in the gamma subdivision of the *Proteobacteria*. In *E. coli*, the *citT* gene coding for the citrate/succinate exchanger (AIT transporter family) is located downstream of the CL genes, while the CitAB two-component signal transduction system is located upstream, on the opposite strand (Table 3). One of the two CL clusters in the genomes of *S. enterica* and *S. enterica* serovar Typhimurium have exactly the same configuration, indicating that they also code for the citrate-to-succinate pathway. Similarly, the AIT transporter gene follows the CL cluster in *Haemophilus influenzae*, *Haemophilus ducreyi*, and *Shigella flexneri*, but a two-component system is absent. On the *H. ducreyi* genome, the transporter is followed by a malic enzyme, the only one found in combination with the CL genes in the *Proteobacteria*. The genome of *E. carotovora* in the gamma subdivision does not contain a decarboxylase clustered with the CL gene, but the associated transporter is from the 2HCT family. The transporter gene is inserted between the CL genes and the genes coding for the CitAB two-component signal transduction system. The transporter is a close homolog of CitW of *K. pneumoniae* (~76% sequence identity; Fig. 1, cluster V), which catalyzes citrate/acetate exchange. Possibly, in this organism the CitW homolog functions as a citrate/succinate, rather than as a citrate/acetate exchanger, and has taken over the role of CitT. The only CL cluster outside the phylum *Proteobacteria* that is devoid of a decarboxylase is found in *L. acidophilus*, a *Lactobacillus* species in the phylum *Firmicutes*. This transporter is from the AIT family, which suggests that the citrate-to-succinate pathway is operative in this gram-positive bacterium. The genes coding for malate dehydrogenase, fumarase, and fumarate reductase are located immediately upstream of the CL genes. *L. plantarum* and other lactobacilli have been reported to produce succinate from citrate (23, 72).

CL clusters containing the OAD type of oxaloacetate decarboxylase genes are as widely distributed as the CL genes, but the actual number of the four genes, *oadABDG*, found in genomes of the different phyla varies. The two divergently transcribed operons coding for the OAD-dependent citrate fermentation pathway in the gamma subdivision of the *Proteobacteria* are found in *P. profundum*, *Salmonella enterica*, *Salmonella enterica* serovar Typhimurium, and *V. cholerae* (44). The operons are extremely well conserved and contain a complete complement of the OAD genes. The associated transporter is the Na^+-citrate symporter in cluster III of the 2HCT transporter family (Fig. 1). A second group of OAD-dependent pathways is found in the *Firmicutes*. The genomes of *Streptococcus mutans*, *Streptococcus pyogenes*, and *E. faecalis* contain the genes *oadA*, *oadB*, and *oadD*, coding for the α, β, and δ subunits of oxaloacetate decarboxylase. In the *Proteobacteria*, the carboxyl transferase α and the biotin-containing carboxyl-accepting δ are two domains of one protein, but in the gram-positive bacteria they form separate proteins. A gene coding for the γ subunit is missing in the gene cluster and is not found elsewhere on the chromosome. The *E. faecalis* cluster contains both an OAD type and a malic enzyme type of decarboxylase. The transporter associated with the pathway in the *Firmicutes* is from the [st301]CITM transporter family in structural class ST[3] in the MemGen classification (TC 2.A.11 CitMHS). Characterized members from this family transport complexes of citrate and divalent metal ions. CitM from *B. subtilis* transports citrate in complex with Mg^{2+}, while CitH transports the complex of citrate and Ca^{2+}. Both transporters are H^+ symporters (65, 66). The citrate fermentation-associated genes in the spirochete *T. denticola* are fragmented into three parts. As in the *Firmicutes*, the OAD cluster contains the genes coding for the α and δ subunits (in one protein) and for the β subunit, but not that coding for the γ subunit. However, no [st301]CITM transporter homolog is encoded on the chromosome. A 2HCT member which is a close relative of BH0400 of *B. halodurans* (Fig. 1, cluster II) is distantly located. Finally, the fusobacterium *Fusobacterium nucleatum* only contains the *oadA* gene in a cluster with a 2HCT transporter.

CL clusters with the gene coding for the malic enzyme (CitM) decarboxylase are found mainly in the phylum *Firmicutes*. The transporters in these clusters are from four different families. The pathways in *L. lactis* and *C. perfringens* involve a 2HCT transporter. *L. plantarum* utilizes a transporter from the AIT family, *E. faecalis* uses a transporter from the CITM family, and *C. tetani* uses a transporter of the [st313]AITC family, which is also found in structural class ST[3]. The substrate specificity of the [st313]AITC transporters is not known. It is unlikely that all these gene clusters represent citrolactic fermentation pathways as present in *L. lactis*. Rather, other metabolic pathways yielding the initial pyruvate product may exist, as is observed for the malate fermentation pathways. On the other hand, the related malolactic fermentation pathway also involves transporters from different families (Table 2). The cluster in *L. plantarum* resembles the cluster in *L. acidophilus*, which does not contain a malic enzyme homolog and is believed to catalyze the conversion of citrate to

succinate (see above). Both clusters contain the necessary enzymes for the latter conversion, suggesting that in *L. plantarum* oxaloacetate may be converted to succinate or to pyruvate. If so, the AIT transporter in the cluster is likely to be involved in the pathway yielding succinate. The existence of two parallel pathways following the action of citrate lyase in the anaerobic breakdown of citrate is observed in other bacteria as well. *E. faecalis* contains both the OAD and CitM-dependent pathways, *H. ducreyi* contains both the CitM-dependent pathway and the citrate-to-succinate pathway, and the *Salmonella* species contain the OAD-dependent and the citrate-to-succinate pathways. The two pathways may not be operative under the same conditions.

Evolutionary states of energy coupling to oxaloacetate decarboxylases. The conversion of citrate to pyruvate is common to the anaerobic breakdown of citrate in bacteria. The conversion involves the splitting of citrate into oxaloacetate and acetate catalyzed by citrate lyase and the decarboxylation of oxaloacetate to pyruvate and carbon dioxide catalyzed by oxaloacetate decarboxylase. The free energy change associated with the conversion is mainly in the latter reaction. While the standard free energy of the reaction catalyzed by citrate lyase is around zero, the standard free energy of the decarboxylation reaction is about −32 kJ/mol, which is comparable to the value for the ATP hydrolysis reaction. In mitochondria, the reverse reaction, the carboxylation of pyruvate, is coupled to ATP hydrolysis by pyruvate carboxylase. It is therefore no surprise that nature has selected the oxaloacetate decarboxylase reaction as the target site for free energy conservation in the pathway from citrate to pyruvate. The oxaloacetate decarboxylases of the CitM type and the OAD type that are involved in the citrate fermentation pathways in bacteria are completely different enzymes, and the two types represent completely different mechanisms of conserving the free energy released in the decarboxylation reaction. The malic enzymes are single-gene products that do not themselves conserve the free energy. Instead, energy conservation is achieved indirectly by "metabolic" coupling to a PMF-generating secondary transporter that takes up the substrate and expels the product of the pathway. In contrast, the OAD complex is a multisubunit complex that directly conserves the free energy by pumping Na^+ across the membrane, thereby generating a sodium ion motive force. It is likely that during evolution the function of energy conservation was added to the decarboxylation reaction catalyzed by a hypothetical primordial oxaloacetate decarboxylase. Different states in evolution may still be recognized in different organisms (Fig. 4).

The primordial oxaloacetate decarboxylases did not conserve the free energy released in the reaction. The primordial malic enzyme type and OAD type of decarboxylases may still be found in *C. perfringens* in the phylum *Firmicutes* and in *F. nucleatum* in the phylum *Fusobacteria*, respectively. The transporters in the CL clusters in these bacteria, CITNcper and FN1375fnuc, form cluster III in the phylogenetic tree, together with the Na^{2+}/citrate symporters of the *Proteobacteria* (Fig. 1). The clustering of the PMF-generating precursor/product exchangers in cluster I of the tree suggests that in *C. perfringens* no free energy conservation takes place in the conversion of citrate to pyruvate. Later in evolution, in other organisms, the transporter evolved or was replaced by a precursor/product exchanger resulting in the energy-conserving pathway as found now in *L. lactis* (Fig. 4A and B). A parallel situation is seen in the fermentation of malate to pyruvate or lactate (Fig. 2A and C). Malic enzymes catalyze oxidative malate decarboxylation in a non-energy-conserving pathway in which the uptake of malate is catalyzed by PMF-driven transporters (cluster IV). The conversion of malate to lactate in the PMF-generating malolactic pathway is accomplished by coupling to a precursor/product exchanger (cluster I). In the genome of *F. nucleatum*, the CL and the 2HCT transporter genes are clustered with an OAD-type decarboxylase gene (Table 2). Only the *oadA* gene, coding for the α subunit of the Na^+-pumping oxaloacetate decarboxylase found in *Proteobacteria*, is present. The α subunit of the OAD complex is responsible for the transfer of the carboxyl group from oxaloacetate to the biotin cofactor on the δ subunit (encoded by *oadD*) (Fig. 3B). Since the latter is not present, it is likely that carbon dioxide is released freely by the α subunit in *F. nucleatum*. Moreover, in the OAD complex the α subunit is peripherally bound to the membrane through a specific interaction mediated by the γ subunit (*oadG*), an integral membrane protein (124, 127). It follows that in *F. nucleatum*, OadA is a cytoplasmic enzyme that does not conserve the free energy released upon decarboxylation of oxaloacetate, in much the same way as the malic enzyme in *C. perfringens* (Fig. 4A and C). The pathways in *F. nucleatum* and *C. perfringens* share a similar transporter for the uptake of citrate (cluster III) and a single-subunit enzyme, but of different origin, for the decarboxylation of oxaloacetate.

Two intermediate states between the single-subunit oxaloacetate decarboxylase in *F. nucleatum* (Fig. 4C) and the energy-conserving OAD complex in the *Proteobacteria* (Fig. 4F) are found in *S. mutans* in the phylum *Firmicutes* (Fig. 4D) and in *T. denticola* in the phylum *Spirochaetales* (Fig. 4E). Energy coupling is achieved by coupling the decarboxylation reaction catalyzed by OadA to a primary transporter that transports Na^+ across the membrane. Na^+ pumping is driven by the decarboxylation of a carboxybiotin group that is carried by a proteinaceous substrate. Essential to the coupling mechanism is that the carboxyl group released from oxaloacetate by OadA is transferred to the carboxyl-carrier protein rather than being released freely. The gene clusters in *S. mutans* and *T. denticola* lack the gene for the γ subunit, leaving the α protein in the cytoplasm. In *S. mutans*, the carboxyl-carrier protein δ is likely to shuttle back and forth between the oxaloacetate decarboxylase α subunit in the cytoplasm and the Na^+ pump β in the membrane. A separate acquisition of the gene coding for the α subunit and for the β-δ pair is evident from their positions in the CL cluster. In *T. denticola*, the genes coding for the α and δ subunits have fused, making α and δ two domains of one protein that shuttles between the cytoplasm and the β subunit in the membrane. Subunit γ was added to the enzyme system, linking the α-δ protein to the transporter in the membrane, resulting in the complex found in *K. pneumoniae*.

PROTEINS

Cloning and Expression

The transport properties of the 2HCT family members were determined by cloning of the structural genes and successful expression in a suitable host organism. The study of a transporter in membranes or cells of the original organism is hampered by the potential presence of other proteins with similar

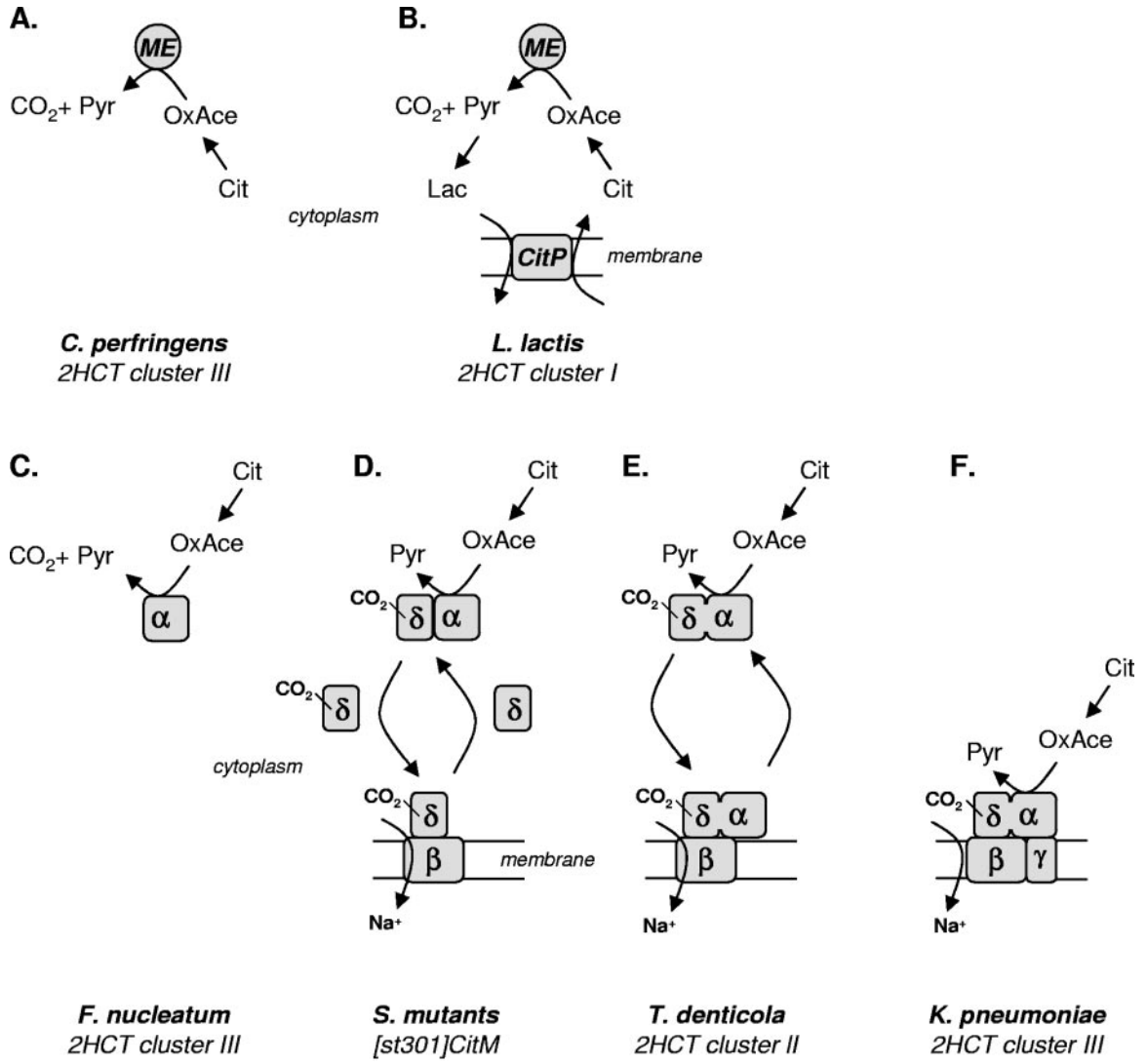

FIG. 4. Energy coupling to oxaloacetate decarboxylation in bacteria. (A and C) Primordial oxaloacetate decarboxylases of the ME type (A) and OAD type (C) do not conserve the free energy released in the reaction. (B) Metabolic coupling. In citrolactic fermentation, the malic enzyme activity drives the exchange of external citrate for internal lactate catalyzed by the 2HCT exchanger CitP, thereby generating membrane potential. (F) Direct coupling. The OAD complex couples the decarboxylation reaction directly to the pumping of Na^+ across the membrane. (D and E) Intermediate evolutionary states of energy coupling by OAD type of decarboxylases. The organisms in which the pathways are found and the transporter involved in the uptake of citrate into the cell are indicated at the bottom. For clusters of the 2HCT family, see Fig. 1. Abbreviations: Cit, citrate; OxaCe, oxaloacetate; Lac, lactate; Pyr, pyruvate. See the text for further explanation.

activities. This may be overcome when the background activity of the organism lacking the transporter can be studied under exactly the same growth and experimental conditions. An example is the citrate/lactate exchanger CitP of *Leuconostoc mesenteroides* 19D. The *citP* gene is located on a plasmid that is spontaneously lost when the cells are grown on rich medium in the absence of citrate. Membrane vesicles prepared from plasmid-free cells (cit^-) grown in the presence of citrate were completely devoid of any citrate transport activity, demonstrating that the activity observed in the cit^+ cells is attributable to CitP in the membrane (94). The transport properties of CitP were studied mostly in membrane vesicles with a right-side-out orientation, which were prepared from *Leuconostoc mesenteroides* cit^+ cells (94). The availability of a well-characterized experimental system is another reason to study transporters in a heterologous expression system. The number of organisms containing members of a particular gene family far exceeds the number of organism that have been characterized in some detail, let alone for which experimental systems such as right-side-out membrane vesicles have been developed. The availability of a right-side-out membrane vesicle system allows the study of the transporter in the absence of subsequent metabolism, which is essential for a kinetic and energetic characterization of the transporter. Routine procedures for the preparation of right-side-out membrane vesicles have been developed for *E. coli* and *L. lactis* (55, 101). The energetic state of the *E. coli* membranes is manipulated by feeding electrons into the endogenous electron transport chain from an artificial electron donor system (ascorbate/

phenazine methosulfate) and, in *L. lactis*, by supplying reduced cytochrome *c* to membranes that were fused to proteoliposomes containing cytochrome *c* oxidase (36). Alternatively, gradients are imposed across the membrane by diffusion potentials, which in the case of *L. lactis* is advantageous, as the fusion step is omitted.

Heterologous expression systems for *E. coli* are abundantly available, and the NICE system, based on the nisin-inducible promoter, has provided a reliable system for expression in *L. lactis* (27, 67). Together, gram-negative *E. coli* and gram-positive *L. lactis* may serve as suitable hosts for genes originating from a wide range of bacteria. *E. coli* is especially suitable for expression of the citrate transporters in the 2HCT family, since the inability to grow on citrate as the sole carbon source under aerobic conditions is due to lack of a citrate transport system in the membrane. Functional expression of a citrate transporter from a recombinant plasmid is immediately evident from growth on citrate or the phenotype on citrate metabolism indicator plates (Simmons agar) (131). Moreover, mutants deficient in malate uptake systems are available that do not grow or grow only poorly on malate, the other main substrate of the transporters of the 2HCT family (25, 75). The genera *Klebsiella* and *Salmonella* are closely related to the genus *Escherichia*, and CitS and CitW of *K. pneumoniae* (58, 126, 143) and CitC of several *Salmonella* serovars (50) were successfully expressed in *E. coli* and characterized. However, CimH and MaeN of *B. subtilis* and MalP of *S. bovis*, more distantly related gram-positive bacteria, could also be functionally expressed in *E. coli* (60, 63, 151). Like that of *Leuconostoc mesenteroides*, the capacity of *L. lactis* to take up citrate is plasmid bound, making plasmid-free strains like *L. lactis* MG1363 good candidates for hosting citrate transporters. Strain MG1363 is deficient in malolactic fermentation because of a defect in the malate/lactate exchanger gene *mleP*. CitP of *Leuconostoc mesenteroides* and MleP of *L. lactis* were functionally expressed in *L. lactis* and then characterized in right-side-out membrane vesicles (7, 9, 10, 11). Introduction of MleP (and CitP) restored malolactic fermentation activity in *L. lactis* MG1363 (J. S. Lolkema, unpublished results). Early attempts to express the citrate/lactate exchanger CitP of *L. lactis* in *E. coli* resulted in poor levels of expression (24, 130), and a more systematic study in which expression vectors and host strains were varied did not result in much improvement (8). Moreover, the latter study suggested that the transporter in *E. coli* and *L. lactis* membranes may have different properties.

Purification and Reconstitution

CitS of *K. pneumoniae* is the only member of the 2HCT family that was purified to homogeneity and reconstituted in proteoliposomes. Following solubilization of membranes prepared from *E. coli* expressing derivatives of the CitS protein, the protein was purified by affinity chromatography. Two types of tags were used. A sequence of six histidine residues (His_6-tag) was engineered at the N terminus of the protein. The biotin acceptor domain (BAD) (the δ domain in Fig. 3B) of the αδ subunit of the oxaloacetate decarboxylase of *K. pneumoniae* was fused to the C terminus of CitS. BAD is a ~10-kDa protein fragment that is biotinylated in vivo when expressed in *E. coli*. The His tag and BAD tag allow for purification on immobilized Ni^{2+}-nitrilotriacetic acid and monomeric avidin resins, respectively (108). A complication with the C-terminal BAD is that the C terminus of the CitS protein is located in the periplasm, which results in less efficient biotinylation of the protein, a reaction catalyzed by biotin ligase situated in the cytoplasm (144). Optimization was sought by coexpressing the *birA* gene, coding for biotin ligase, and by adding biotin to the growth medium (56). The yield of the procedure was further improved by replacing the His_6 tag with a His_{10} tag (109), by moving the BAD domain from the C to the N terminus (109), and by using different expression systems, growth conditions, and host strains (56). These improvements resulted in yields of as much as 6.5 mg of pure protein from 1 liter of culture for the His_{10}-tagged CitS protein. Purified His-tagged CitS showed a higher mobility, corresponding to a protein with a molecular mass of 33 kDa on sodium dodecyl sulfate-polyacrylamide gel electrophoresis (SDS-PAGE), than the expected 47 kDa. An aberrant mobility is normal for membrane proteins and is due to the larger amount of SDS binding to these hydrophobic proteins compared to the average amount bound by the globular proteins used as standards. The BAD-tagged proteins undergo proteolytic cleavage of the BAD domain at the fusion sites, which is evidenced by the appearance of two equally stained bands after SDS-PAGE, one corresponding to the BAD-CitS fusion protein and one to CitS. The copurification of tagged and untagged CitS was taken as evidence for an oligomeric structure of the protein (see "Quartenary Structure" in "STRUCTURE" below) (108). Purified CitS was used for mechanistic studies following reconstitution in proteoliposomes (56, 109) and for single-molecule fluorescence spectroscopy studies (57).

The procedure for the reconstitution of CitS of *K. pneumoniae* in protein-free liposomes was first developed using solubilized membranes prepared from *K. pneumoniae* grown under anaerobic conditions (30). Although interference of other proteins cannot be excluded, the resulting proteoliposomes showed the main transport characteristics of the CitS protein. Later, the solubilized membranes were replaced by purified CitS, resulting in a liposomal system containing essentially one membrane protein. Purified CitS in dodecylmaltoside solution was reconstituted by dilution into a suspension of preformed liposomes made of soybean phosphatidylcholine (56, 108, 109). Kinetic analysis of citrate transport catalyzed by CitS suggested that the protein was inserted asymmetrically in the liposomal membrane (109).

More recently, small-scale purification methods were developed for members of the 2HCT family strictly for analytical purposes (64, 135, 136). The purification method is based on Ni^{2+}-nitrilotriacetic acid affinity chromatography and yields enough protein for visualization by SDS-PAGE. This method was used in labeling studies of single-Cys mutants of CimH of *B. subtilis* (63) and CitS of *K. pneumoniae* (135, 136).

STRUCTURE

Primary Structure

Superfamilies and structural classes. Secondary transporters are widely distributed in nature. As a result, the transporters have a great sequence diversity, and to date, the TC system (http://www.tcdb.org) developed by Saier and coworkers lists some 85 families in the porters (uniporters, symporters, and

antiporters) category (17, 117). Many families are grouped together in superfamilies when distant evolutionary relationships are detected between members of different families. Well-known examples are the MFS, the amino acid-polyamine-organocation superfamily, and the ion transporter superfamily (52, 111, 118). The TC system is based on sequence relatedness. Distant evolutionary relationships between sequences belonging to different families are identified by comparing the similarity of the two sequences before and after randomizing the sequences. Homology is established when the sequence identity is at least 9 standard deviations away from the average obtained with 500 random shuffles. Using this criterion, the 2HCT family was not shown to be related to any other family in the TC system. The 2HCT family corresponds to the citrate-cation symporter (TC 2.A.24) family in the TC system (113).

A different approach for establishing distant evolutionary relationships between families of membrane proteins involves hydropathy profile alignment (79). The approach is based on the fact that during evolution the structure of a protein is much better conserved than the amino acid sequence. Consequently, proteins grouped in a family based on sequence identity also share a similar fold, and comparing the structures of proteins enables the detection of more distant evolutionary relationships than is possible by sequence comparison. Due to their architecture, proteins that reside in the plasma membrane have characteristic hydropathy profiles which are a "fingerprint" of their structure (68). In this approach, the hydropathy profile is used to estimate structural similarity between membrane proteins and replaces the actual structure in the search for evolutionary relationships. The procedure involves computation of the optimal alignment of two averaged family hydropathy profiles. The difference between the optimal aligned profiles is compared to the average difference between the individual profiles and the average profile in each family. This provides a statistical criterion for structural similarity and, therefore, for an evolutionary relationship. Using this approach, the 2HCT family was shown to be related to 31 other families of membrane proteins (80, 81). The 32 families are contained in structural class ST[3] in the MemGen database (http://molmic35.biol.rug.nl/memgen/main.htm). The implication is that all proteins in ST[3] share a similar fold. The wider scope of the hydropathy profile comparison method versus the sequence comparison method is evident from the inclusion of the complete ion transporter superfamily from the TC system in structural class ST[3]. In addition, ST[3] contains a number of families which, like the 2HCT family ([st326]2HCT), are completely unrelated in sequence. All characterized transporters in ST[3] are either organic/inorganic anion transporters or Na^+/H^+ antiporters.

Sequence analysis. The amino acid sequences of the members of the 2HCT family vary in length between 421 and 456 residues, with the exception of the two *Onion yellows phytoplasma* sequences, which are both considerably shorter, with 371 and 381 residues. *Onion yellows phytoplasma* is a plant pathogen belonging to the class *Mollicutes*, containing many minimal life forms. They live in insects and plants and are characterized by a highly degenerative genome. The *Onion yellows phytoplasma* genome contains only 860 kbp, which code for no more than 754 proteins. The CitS and CitS_1 sequences of *Onion yellows phytoplasma* are the most distant sequences in the family (Fig. 1). A multiple-sequence alignment shows that the sequences are truncated at the N terminus by some 100 residues. The hydropathy profile over the multiple-sequence alignment reveals two or three hydrophobic peaks in this region, suggesting that the *Onion yellows phytoplasma* transporters would miss at least two N-terminal transmembrane segments (Fig. 5A). Even though it would be quite coincidental that two similarly truncated transporter proteins are found in the same genome, it remains to be demonstrated that the two genes code for functional transporters.

The amino acid composition and average hydropathy profile of the 2HCT family are typical for integral membrane proteins: a high fraction of hydrophobic residues are clustered, resulting in a peak pattern in the hydropathy profile (Fig. 5A). The N terminus is hydrophilic, the C terminus hydrophobic. A hydrophilic region around position 300 separates seven hydrophobic regions in the N terminus from five hydrophobic regions in the C terminus (see below). Leucine is the most abundant residue in the family (13% of the residues), followed by isoleucine, alanine, and glycine, each accounting for 10% of the residues. Only 15 positions in the alignment are completely conserved: 10 glycine residues, 2 proline residues, 1 leucine residue, 1 isoleucine residue, and 1 arginine residue. The conserved arginine plays a critical role in catalysis. A less strict comparison by scoring the fraction of identical pairs at each position in the alignment (pairwise sequence identity profile) (Fig. 5B) identifies three regions that are particularly well conserved in the family. These are two narrow regions corresponding to the fourth and sixth hydrophobic regions (around positions 150 and 225, respectively) and a broader region just in front of the C terminus. The latter region contains the conserved arginine residue.

Domain structure. Early studies (45) recognized that many of the structural genes coding for transporters of the major facilitator superfamily contain a repeat in the two halves of the gene, implying that they arose from an ancient gene duplication. The proteins would have consisted of two domains with similar structures. A low-resolution structure of the oxalate transporter OxlT of *O. formigenes* (46) and the recent high-resolution structures of the lactose transporter LacY (2) and the glycerol-3-P transporter GlpT (47) of *E. coli*, all MFS members, clearly revealed the two domains, each consisting of six transmembrane segments and with superimposable structures. The two domains are connected by a hydrophilic linker that shows up as a "dip" in the hydropathy profile and separates the N-terminal domain from the C-terminal domain. A similar "dip" is observed in the profiles of structural class ST[3] family profiles (around position 300 in Fig. 5A for the 2HCT family), suggesting a similar two-domain structure, but sequence identity between the N- and C-terminal halves is not evident.

Sequence homology between the N- and C-terminal halves of the proteins in the different families of structural class ST[3] was searched for by use of the BLAST algorithm (4). It was demonstrated that the N-terminal (or C-terminal) halves "hit" a C-terminal (or N-terminal) half with a significantly higher frequency than the proteins in a control set of the same length and amino acid composition taken from unrelated transport protein families. Most of the Expect values of the hits, which provide a measure of significance, were high, indicating a weak relationship. Remarkably, most hits were observed between the

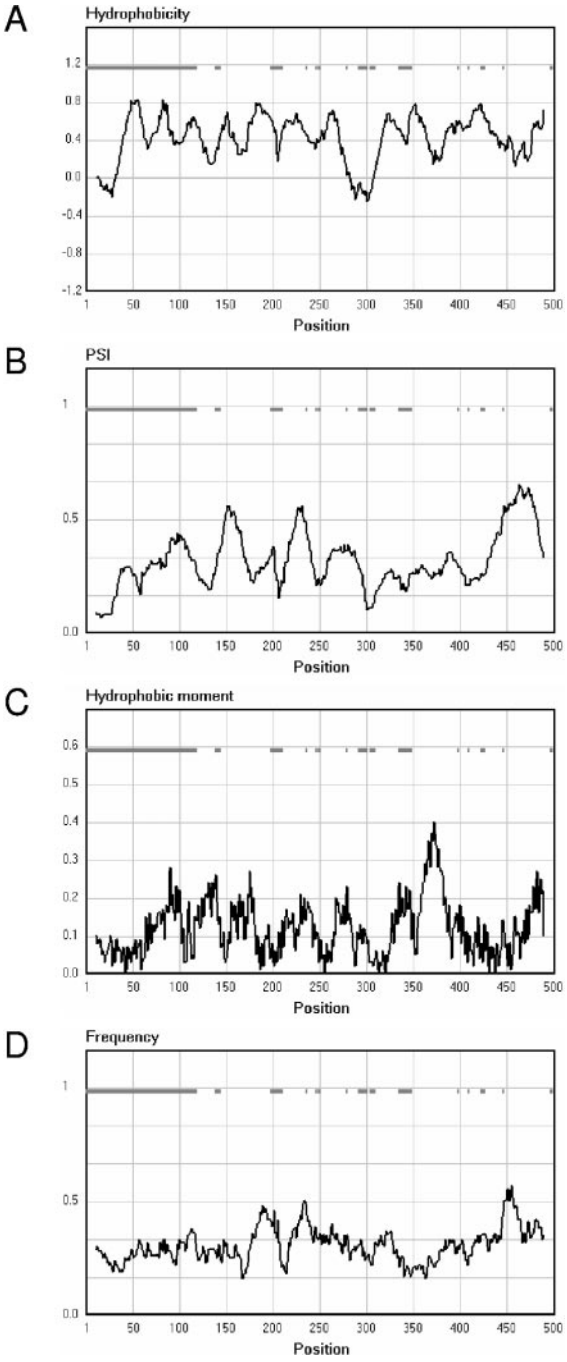

FIG. 5. Profile analysis of the 2HCT family of transporters. The profiles were calculated based upon a multiple-sequence alignment of the "typical" sequences listed in Table 1, using a window of 20 residues (see also the legend to Fig. 1). Bars in the tops of the panels indicate the positions of gaps in the sequences. (A) Hydropathy profile using the Eisenberg scale (38). (B) Pairwise sequence identity (PSI) profile. The fraction of identical pairs at each position averaged over the window is plotted. (C) Hydrophobic moment profile. The hydrophobic moment was calculated at a periodicity of 100° (α-helix). (D) Frequency distribution of the glycine, alanine, and serine residues.

N- and C-terminal halves of different proteins, rather than the same protein. Analysis of the best-scoring local alignments showed that the homologous region involved the complete N- and C-terminal parts, consistent with two homologous domains (82).

The number of hits between N-terminal and C-terminal halves of the 2HCT family of transporters was small. The longest local alignment was observed between the N-terminal half of FN1375 of *F. nucleatum* and the C-terminal half of NP973298 of *T. denticola*. The span of 148 positions with 29% sequence identity covered 60 and 70% of the N- and C-terminal sequences, respectively. A higher sequence identity of 33% was observed in a span of 78 positions between the N- and C-terminal halves of BH0400 of *B. halodurans*. All local alignments involved more or less corresponding parts of both halves. A multiple-sequence alignment of the N- and C-terminal halves of these best-hit scoring sequences revealed a single sequence motif, GGxG, just in front of position 210 in the alignment (Fig. 6). In the multiple-sequence alignment of all 2HCT family members, the motif is completely conserved in the C-terminal half and almost fully conserved in the N-terminal half (Fig. 7). In the latter half, the motif is violated by the two truncated *Onion yellows phytoplasma* sequences. The motifs are at the center of the conserved regions around positions 225 and 460 (Fig. 5B). The alignment of the N- and C-terminal halves shows that, except for the two regions containing the GGxG motif, the hydrophobic regions coincide in the two halves. However, the first hydrophobic region in the N-terminal domain does not have a counterpart in the C-terminal domain (see below).

Membrane Topology

Transmembrane segments. The average hydropathy profile of the 2HCT family, shown in Fig. 5A, predicts the presence of 12 transmembrane segments following the hydrophobic regions which are long enough to span the membrane. A secondary structure prediction by the TMHMM program (62) results in 10 to 13 transmembrane segments for the different members in the family when the two *Onion yellows phytoplasma* sequences are not taken into account (see above). Experimental studies of the membrane topology of CitS of *K. pneumoniae* using site-directed Cys labeling, alkaline phosphatase (PhoA) fusions, insertions of reporter proteins, and insertion in an in vitro translation/insertion system showed that only 11 of the hydrophobic regions were transmembrane. A conserved 12th region, Vb, around position 220 (Fig. 5A and B), is exported into the periplasm (Fig. 8). This membrane topology is believed to apply to all other members in the family (144–146, 148).

The exclusion of predicted hydrophobic segment Vb was first demonstrated by the PhoA reporter fusion technique in *E. coli* (90). N-terminal fragments of the CitS protein were fused to the reporter enzyme alkaline phosphatase (PhoA) devoid of its signal sequence (144). *E. coli* PhoA is a periplasmic enzyme which becomes active only following maturation in the oxidative environment of the periplasm. Fusion of PhoA at the hydrophilic regions of a membrane protein residing in the periplasm is assumed to export the PhoA moiety outside the cell, resulting in an active enzyme. In contrast, fusion to hydrophilic regions that reside in the cytoplasm prevents maturation by retaining the enzyme in the cytoplasm. A series of CitS-PhoA fusions localized the large hydrophilic region at around position 300 in the cytoplasm. This was consistent with the six TMSs in the preceding N-terminal half of the protein shown in Fig. 8. Fusions to sites flanking hydrophobic region Vb showed high PhoA activity, plac-

FIG. 6. Multiple-sequence alignment of N- and C-terminal domains of selected members of the 2HCT family. N-terminal halves of sequences that produced hits with C-terminal halves, and vice versa, were selected, and a multiple sequence alignment was produced with CLUSTAL W (141). The overall sequence similarity between the two groups of five N-terminal (top) and C-terminal (bottom) halves is indicated with an asterisk for identical residues and with a tilde for similar residues. The positions of the putative TMSs in the N- and C-terminal halves are indicated by solid lines above and below the sequences, respectively. Similarly, the positions of the conserved regions, Vb and Xa, are indicated by dotted lines.

ing the region in the periplasm. Remarkably, the same series of fusions identified only segments VII, X, and XI in the C-terminal half as transmembrane; fusions to the AH region resulted in high PhoA activity, thereby placing segments VIII and IX in the periplasm. The use of PhoA as a periplasmic reporter led to the first topology model of CitS, with only 9 of the 12 hydrophobic regions being inserted into the membrane and the remaining 3 regions in the periplasm (144). The model was partially confirmed and partially disproved by an insertion study of CitS in the endoplasmic reticulum membrane, using dog pancreas microsomes in an in vitro translation/insertion system (148). Topological information was obtained from the glycosylation activity in the lumen of the microsomes. The *E. coli* membrane protein leader peptidase (Lep) was used as an insertion vehicle by replacing its second transmembrane segment with different fragments of the CitS protein. The catalytic peptidase domain that is glycosylated in the lumen of the microsomes is downstream of the inserted fragment. Glycosylation provides an assay for successful translocation of the domain across the microsomal membrane and, therefore, of the insertion capacity of the fragment (for a review, see reference 147). The 12 hydrophobic regions in the CitS polypeptide,

FIG. 7. Sequence logos of the region around the sequence motif GGxG (positions 5, 6, and 8) in the N-terminal (top) and C-terminal (bottom) domains of the 2HCT transporters. The multiple-sequence alignment included all typical sequences (see Fig. 1 and Table 1). The logos were generated using WebLogo, version 2.8.1 (http://www.bio.cam.ac.uk/cgi-bin/seqlogo/logo.cgi).

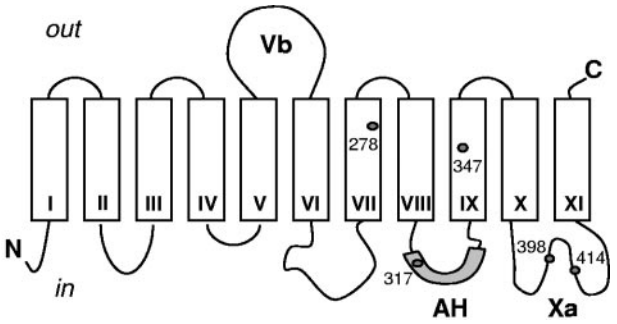

FIG. 8. Topology model of the members of the 2HCT family, based on experimental data for CitS of *K. pneumoniae*. Boxes represent putative transmembrane segments. The lengths of the loops correlate with the numbers of residues present in the loops. Segment Vb corresponds to a hydrophobic region that was predicted to be transmembrane. Loop Xa is one of the best-conserved regions in the 2HCT family and folds as a pore-loop structure. The AH loop folds into an amphipathic surface helix. The positions of the five endogenous cysteine residues Cys 278, Cys317, Cys347, Cys398, and Cys414 in CitS of *K. pneumoniae* are indicated by dots.

including Vb, VIII, and IX, inserted into the membrane on their own. However, in the presence of the preceding TMSs of the CitS protein, region Vb was translocated to the lumen of the microsomes, as was observed in the bacterial insertion system. In contrast, TMSs VIII and IX formed an additional pair of TMSs during insertion into the endoplasmic reticulum membrane. Apparently, the bacterial and eukaryotic insertion machineries interpret the topological information in the truncated CitS polypeptide chains in slightly different ways, resulting in models with 9 and 11 TMSs, respectively (148). The discrepancy between the two models was resolved by a study of insertion of the full-length CitS protein into the *E. coli* membrane. This study demonstrated that the exclusion of TMS VIII from the membrane in the truncated protein was a folding artifact (145). Accessibility of a cysteine residue in the loop between TMSs VIII and IX positioned the loop in the cytoplasm in the full-length protein. The cysteine residue moved from the periplasm to the cytoplasm when the truncated CitS protein containing TMSs I to VIII was extended with TMS IX. It was concluded that TMS IX is required for proper insertion of segment VIII (see below).

The topology of CitS with the 11 TMSs was confirmed by inserting the 10-kDa BAD of the oxaloacetate decarboxylase of *K. pneumoniae* (21, 28) or six consecutive histidine residues (His tag) in specific loops of the full-length protein. The localization of the tag was then determined (146). At many sites, the protein tolerated the insertion and was still active in citrate transport, thereby confirming the correct folding of the protein. A cytoplasmic localization of the BAD follows from the presence of the biotin cofactor bound to the domain, requiring posttranslational modification by biotin ligase, an endogenous enzyme present in the cytoplasm of *E. coli* (22). Biotinylation is easily detected with alkaline phosphatase-labeled streptavidin. His-tagged mutants were treated in spheroplasts by proteinase K, which digests tags located at the periplasmic side of the membrane but leaves cytoplasmically located tags intact. The latter were detected by immunoblotting using antibodies raised against the His tag. Insertions and fusions of the BAD confirmed the cytoplasmic location of the N terminus, the loops between TMSs VI and VII and between TMSs X and XI, and the periplasmic location of the C terminus (146). A His tag insertion confirmed the localization of the Vb loop in the periplasm. Support for the cytoplasmic location for the AH and Xa loops (Fig. 8) was obtained by labeling of endogenous or engineered cysteine residues in the loops. Two native cysteine residues located in the Xa region were shown to be inaccessible from the periplasm with the membrane-impermeative reagent AmdiS (4-acetamido-4′-maleimidylstilbene-2,2′-disulfonate) but were readily accessible from the cytoplasm (135). The same results were obtained for a series of engineered cysteine residues in loop AH (see below) (136).

Amphipathic helix and membrane insertion. The cytoplasmic loop between TMSs VIII and IX in CitS forms an amphipathic surface helix which is proposed to play a role in the atypical insertion of TMSs VIII and IX (145). Insertion of truncated versions of CitS, comprising TMSs I to VIII, into the bacterial membrane showed that TMS VIII (around position 350 in Fig. 5A), which is one of the most hydrophobic transmembrane segments of CitS, resided in the periplasm and did not insert into the membrane. Insertion was induced when the truncation was extended to contain the next TMS, TMS IX (around position 390 in Fig. 5A), which is the least hydrophobic TMS in the protein. Apparently the presence of TMS IX is both essential and sufficient for proper insertion of both segments (145). It was proposed that hydrophobic segment VIII would drive the insertion of the VIII/IX helix pair into the membrane and that the truncation up to TMS VIII would represent a trapped folding intermediate in a nonsequential insertion mechanism. During cotranslational insertion of CitS, the part of the nascent chain containing both segments VIII and IX would first be exported to the periplasm, and only when both segments are completely synthesized would the hydrophobicity of TMS VIII facilitate the insertion of TMS IX (145, 147).

Profiles of the hydrophobic moment revealed a strong amphipathic character of the cytoplasmic loop between TMSs VIII and IX, when folded as an α helix (Fig. 5C), suggesting that the loop might form a surface helix (AH) (Fig. 8). This property is conserved in all members of the 2HCT family and

throughout structural class ST[3] in the MemGen classification. Cysteine-scanning mutagenesis was used to study the secondary structure of the AH loop in CitS of *K. pneumoniae*. CitS derivatives containing single cysteine residues at 20 successive positions in the loop were labeled with the fluorescent probe fluorescein-5-maleimide in membrane vesicles with an inverted orientation (inside-out membranes). The labeling showed a clear periodicity in the accessibility of the 20 positions. Residues predicted to be at the hydrophobic face of the putative α-helix were not accessible to the label, whereas those at the hydrophilic face were easily accessed and labeled. Pretreatment of whole cells and inside-out membranes expressing the mutants with the membrane-impermeative thiol reagent AmdiS confirmed the cytoplasmic localization of the AH region. Cysteine residues at the hydrophilic face were accessible for labeling with AmdiS only from the cytoplasmic side of the membrane (136).

The presence of the amphipathic structure is believed to play a role in the insertion mechanism of the TMS pair VIII and IX. Studies done with the Tsr chemoreceptor protein of *E. coli* showed that introduction of mutations into an amphipathic stretch of 11 residues in a cytoplasmic loop immediately downstream of a transmembrane segment, affected the insertion process. A correlation was observed between the export of the cytoplasmic loop and the amphipaticity of the stretch. It was suggested that an amphipathic sequence might represent a determinant of membrane topology (128). A similar function was then proposed for the CitS AH region, where it would be involved in proper insertion of the protein into the membrane, possibly by stabilizing the folding intermediate with TMS VIII in the periplasm (136).

Pore-loop structure. The cytoplasmic loop between TMSs X and XI is one of the best-conserved regions in the proteins of the 2HCT transporter family. Experimental evidence has been presented for two transporters, CitS of *K. pneumoniae* and CimH of *B. subtilis*, showing that the loop may form a so-called pore-loop or reentrant loop that is part of the translocation site (64, 135). A pore-loop structure is formed by part of a loop which is folded back in between the TMSs. Pore-loops are commonly found in channel proteins, where they function as selectivity filters, but the recent structure of the glutamate transporter homolog of *P. horikoshii*, Glt_{Ph}, revealed that they may be essential features of secondary transporters as well (154). Known channel structures and the Glt_{Ph} transporter show that at least two pore-loops are found together in the structure. For example, potassium channels are tetrameric structures with four pore-loops (one on each subunit), which enter the pore formed by the TMSs from the same side of the membrane (*cis* pore-loops) to form a pathway for potassium ions (34). In aquaporins (39, 99) and the glutamate transporter, two pore-loops in one polypeptide chain enter the membrane-embedded part of the structure from opposite sides of the membrane (*trans* pore-loops), where they meet in the 3D structure. Pore-loop structures are not easily predicted by computational methods. In the hydropathy profiles of proteins known to form pore-loops, they show up as moderately hydrophobic regions (132).

Without the availability of a 3D structure, pore-loop structures are experimentally identified in a membrane protein by accessibility studies. In general, a region of a loop that folds back in between the TMSs is detected by the accessibility of residues in the loop from the opposite side of the membrane. Often, pore-loops are characterized as regions in putative loops that are accessible from both sides of the membrane. This property may be related to their presumed function in the translocation mechanism (42, 43, 133). The CitS protein of *K. pneumoniae* contains five native cysteine residues, and two of them, Cys398 and Cys414, are located in cytoplasmic loop Xa (Fig. 8). Labeling of both residues with the membrane-impermeative thiol reagent AmdiS indicated a cytoplasmic localization of the Xa region, since they were accessible to the reagent only in inside-out membranes and not in whole cells. However, when small impermeable reagents (e.g., MTSET {[2-(trimethylammonium)ethyl]methanethiosulfonate bromide}) were used, the cysteine residues at positions 398 and 414 were accessible from the periplasmic as well as from the cytoplasmic side of the membrane. The experiment indicated that an access pathway for small molecules exists from the periplasm to both residues in the cytoplasmic loop (135). Similarly, in the CimH protein of *B. subtilis*, cysteine residues engineered at positions 420 and 428 of the Xa region were accessible to impermeative MTSES (2-sulfonatoethyl-methanethiosulfonate) from the periplasmic side of the membrane (64). Protection of the cysteine residues in the Xa region against attack from the periplasmic side of the membrane by substrate and/or co-ion emphasized the involvement of the pore-loop structure in the binding and translocation mechanism in both proteins.

Using similar approaches, pore-loop structures were proposed for members of the glutamate transporter family (DAACS, TC 2.A.23). Studies of GltT of *Bacillus stearothermophilus* and GLT-1, found in the central nervous system, identified the presence of two pore-loop structures. One of the loops penetrated the membrane-embedded part of the protein from the cytoplasm (43, 133) and the other from the periplasm (42). In the glutamate transporters, the pore-loop entering from the cytoplasm was shown to be accessible to the larger AmdiS reagent from both sides of the membrane. This suggests a different access pathway, based on size, or a pore-loop that penetrates all the way to the other side of the membrane. Recently crystallized Glt_{Ph}, a homolog of GltT and GLT-1, confirmed the presence of the two pore-loops in the structure, demonstrating that the biochemical experimental approaches enable the correct prediction of pore-loops (154). Pore-loop structures have been proposed to be present in the members of the Na^+/Ca^{2+} exchanger family (CaCA, TC 2.A.19) (51, 100, 112), the phosphate exchanger (71), and the melibiose transporter MelB of *E. coli* (GPH, TC 2.A.2) (32).

Structural Model

Combining the available data results in the structural model for the proteins of the 2HCT family depicted in Fig. 9 (82). The proteins contain two homologous domains consisting of five TMSs each and separated by a large hydrophilic loop that resides in the cytoplasm. The two domains consist of TMSs II to VI and VII to XI; TMS I is not part of the two-domain structure. The distribution of the TMSs over the two domains follows from three lines of evidence. (i) Many families in structural class ST[3] contain 10 TMSs. Average hydropathy profile alignments of these transporter families show an additional TMS I in 2HCT (80, 82). (ii) The multiple-sequence alignment of the N- and C-terminal

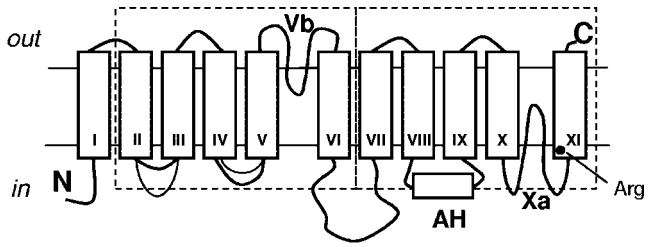

FIG. 9. New structural model for the members of 2HCT transporter family. Two homologous domains containing five TMSs each, with an inverted topology in the membrane, are surrounded by dashed boxes. The two domains contain a pore-loop structure and enter the membrane-embedded part of the protein from the periplasmic or cytoplasmic side of the membrane, respectively (Vb and Xa). AH represents an amphipathic surface helix. The position of the conserved arginine residue in TMS XI is indicated by a black dot.

halves of the 2HCT members shows no segment corresponding to TMS I in the C-terminal domain (Fig. 6). (iii) Finally, the highest sequence identity between the two domains is observed in a stretch of 78 residues in BH0400 of *B. halodurans*, corresponding to TMS V plus Vb in the N-terminal domain and TMS X plus Xa in the C-terminal domain. Assuming that the domains represent continuous structural entities, it follows that TMS I forms a separate domain by itself. A major consequence of the odd number of TMSs in the two domains is that they have opposite orientations in the membrane. The N terminus of the N-terminal domain is in the periplasm, while the N terminus of the C-terminal domain is in the cytoplasm. Homologous domains with inverted topologies may turn out to be a common structural motif in membrane proteins, since they are found in the 3D structures of aquaporins, the ammonium transporter AmtB and the Na^+/H^+ antiporter NhaA of *E. coli*, and the leucine transporter LeuT of *A. aeolicus* (39, 49, 61, 99, 153) and have been proposed for a number of other proteins based on biochemical evidence and sequence analysis (51, 53, 100, 112, 116). The domain structure in the model indicates that regions Vb and Xa are corresponding loops. Sequence homology indicates a similar folding, strongly suggesting that region Vb folds into a pore-loop structure. Similarities between regions Vb and Xa are as follows: (i) both regions are hydrophobic but not transmembrane (Fig. 5A), (ii) both regions are well conserved (Fig. 5B), (iii) the sequence motif GGxG is located in both regions (Fig. 6 and 7), and (iv) both regions contain an extraordinarily high fraction of residues with small side chains, G, A, and S (Fig. 5D). The last item may reflect a compact packing of the loops between the transmembrane segments. The sequence motif GGxG is located at the center of the conserved regions and may represent the vertex of the loops (Fig. 7). The amphipathic surface helix AH in the C-terminal domain does not seem to have its counterpart in the N-terminal domain (Fig. 5C). This may be related to the proposed function of the segment in the insertion of the protein in the membrane during biogenesis. The opposite membrane topology will have set different constraints on the insertion mechanisms of the two domains, which may have resulted in divergent structural evolution of these corresponding parts of the sequences.

The two pore-loops entering the protein from opposite sites of the membrane (*trans* pore-loops) resemble the crystal structure of the glutamate transporter homolog Glt_{Ph}. The glutamate transporters contain 8 TMSs, with the cytoplasmic pore-loop between TMSs VI and VII and the extracellular pore-loop between TMSs VII and VIII (154). In the three-dimensional structure, the two pore-loops are in close contact. The structural model for the 2HCT family, with the inverted membrane topology of the two homologous domains and the two pore-loop structures entering the protein from opposite sites of the membrane, resembles the structure of the aquaporin water and glycerol channels (39, 99) and the putative structure of a family of Na^+/Ca^{2+} exchangers, NaCX (51, 100, 112). Aquaporins consist of two homologous domains of three TMSs, each with pore-loops between the second and third TMS in each domain. As in the glutamate transporters, the two pore-loops are in close proximity and form the permeation pathway. Like the 2HCT transporters, the NaCX exchangers are believed to be built of two domains of five TMSs. However, the pore-loops are between the second and third TMSs in each domain rather than between the fourth and fifth as in the 2HCT family (137). Possibly these structural variations represent similar translocation mechanisms.

Quaternary Structure

Three lines of evidence indicate that the 2HCT transporter CitS of *K. pneumoniae* exists as a multimeric structure, probably a homodimer. The enzyme solubilized in Triton X-100 was shown to run as a dimer on blue native PAGE (57, 150). Purification of BAD-tagged CitS produced from a recombinant plasmid strongly suggested the dimeric structure of the protein (see "Purification and Reconstitution" in "PROTEINS" above) (108). The BAD-CitS fusion protein was purified from other membrane components by affinity chromatography by binding of the biotin group of BAD to immobilized avidin. Analysis of the protein preparation following elution from the column by SDS-PAGE revealed two products, one corresponding to the BAD-CitS fusion and the other to CitS. The size of the BAD (~10 kDa) allowed discrimination between the two proteins on SDS-PAGE. The result indicated that (part of) the protein population that specifically bound to the avidin resin was a heterodimer of BAD-CitS and CitS, indicating a strong interaction between CitS monomers. It was unclear how the BAD was removed from the untagged CitS molecules.

Finally, strong evidence for the existence of the homodimeric association state of CitS was provided by single-molecule fluorescence spectroscopy of purified CitS (57). Labeling of purified CitS at the position of cysteine residue Cys394 in region Xa with two different fluorophores (Alexa Fluor 546 and 568) produced a population of CitS dimers with both fluorophores attached. The colocalization of the two fluorophores could be demonstrated by the consecutive two-step bleaching of a single fluorescence spot and the associated change of the dichroic ratio upon bleaching of the first fluorophor.

MECHANISMS

Kinetics

Symport and exchange. The catalytic cycle of a secondary transporter that catalyzes the transport of a substrate in sym-

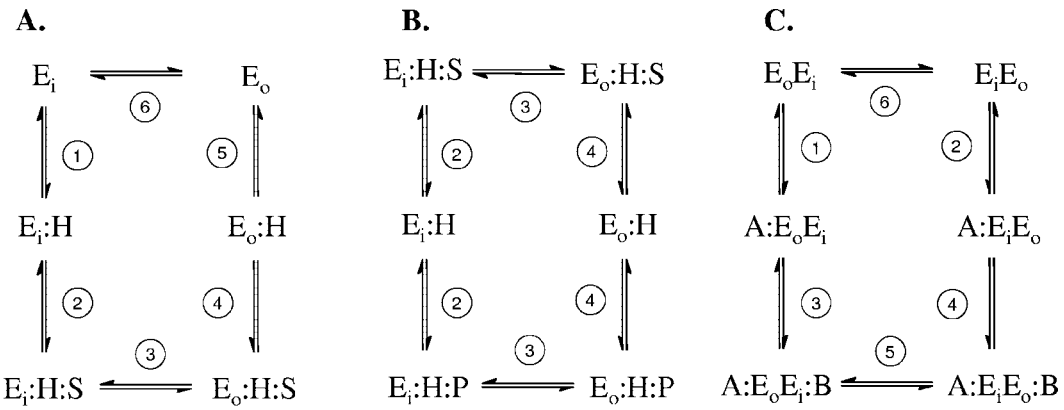

FIG. 10. Kinetic schemes representing mechanisms of a symporter (A), a symporter in the exchange mode (B), and an antiporter (C). E represents the transporter. The subscript i and o indicate the orientation of the binding sites toward the cytoplasm and periplasm, respectively. The antiport mechanism in panel C assumes a dimer of two transporter molecules with one binding site oriented to the periplasm and the other to the cytoplasm. H, proton; S, substrate; P, product; A and B, two substrates at different sides of the membrane.

port with a proton requires a minimum of six steps and six kinetic states (Fig. 10A). In the steps 1 and 2, H^+ and substrate in the external medium bind to sites on the transporter protein, forming a ternary complex. Isomerization of the transporter protein reorients the "loaded" binding sites, now facing the cytoplasm (step 3). Subsequently, H^+ and substrate dissociate from the protein into the cell interior (steps 4 and 5), and reorientation of the "empty" binding sites to the external medium completes the catalytic cycle (step 6). Coupling of the translocation of proton and substrate is achieved by allowing only the "fully loaded" and "free" transporter molecule to reorient the binding sites (steps 3 and 6). Binding of either substrate or proton to the "free" transporter inhibits the isomerization step. Failure to do so results in a (partial) uncoupling of the two fluxes. Similarly, binding of substrate to the binary complex relieves the inhibition of isomerization. Additional states in the scheme are necessary when the binding/dissociation of substrate and proton proceed in random order and for different substrate/co-ion stoichiometries. The kinetic scheme applies equally well to proton symport, sodium ion symport, or a combination of the two, and indeed, the 2HCT transporter family contains all these types (Table 1). Mechanistically, these different modes of energy coupling are similar, and they most likely represent only minor details in the structure of the proteins. The cation-to-substrate ratio does not affect the kinetics of the transporter but determines the thermodynamic force on the transport reaction in terms of the accumulative power of the transporter. The proton motive force and/or sodium ion motive force together with the transport stoichiometry and the charge of the substrate determine the accumulation of the substrate under conditions of thermodynamic equilibrium. The chemical H^+/Na^+ gradient affects the kinetics of the transporter indirectly through the association and dissociation kinetics of external and internal H^+/Na^+ concentrations. In cases where net charge is translocated across the membrane, the membrane potential, which is general to the proton and sodium ion motive forces, affects one or more rate constants in the scheme. The effect of the membrane potential may be an electrophoretic movement of the co-ion or charged substrate in the access pathway to or from its binding site or the movement of a fixed charge on the protein in the electrical field across the membrane. The fixed charge could be a charged side chain on the protein which is neutralized by bound substrate or co-ion, or carried by the substrate or co-ion bound to the transporter. For the 2HCT transporters to be electrogenic, the negatively charged 2-hydroxycarboxylate substrates require the number of cotransported ions to be one higher than the valence of the anion. CitS of *K. pneumoniae* is believed to transport the divalent form of citrate, $Hcit^{2-}$, in symport with two Na^+ ions and one H^+ ion (see "Transport Properties" in "FUNCTION" above). Binding of the substrate and co-ions to the transporter may result in the formation of a ternary complex with a single net positive charge. The membrane potential will then exert its kinetic effect in steps 1 to 5. Alternatively, the "unloaded" transporter protein bears a net negative charge of one unit, resulting in a neutral ternary complex. Then, the membrane potential effects step 6.

The exchange of internal and external substrate is a partial reaction of the symporter reaction depicted in Fig. 10A. It is believed that the 2HCT exchangers, CitP and MleP, of lactic acid bacteria catalyze exchange by utilizing this mechanism (Fig. 10B) (94). Exchange involves binding of substrate at one side of the membrane to the protonated transporter (step 2, up), followed by reorientation of the binding site (step 3) and dissociation into the cytoplasm (step 4). A high concentration of substrate in the cytoplasm may result in a reversal of these steps, thereby translocating a substrate molecule in the opposite direction. Transporters such as CitP and MleP have broad substrate specificity, and the availability of different substrates at the two sides of the membrane results in the exchange of substrate molecules between the two pools. External citrate (CitP) or malate (MleP) is exchanged for internal lactate. In the symport mechanism, exchange competes with full turnover, depending on the concentrations of substrate at the two sides of the membrane. The exchange mode is an inherent property of the symport mechanism. Exchange differs from the antiport mechanism (see below) in that the movement of a substrate molecule in one direction is not mechanistically coupled to the movement of a substrate molecule in the opposite direction. The 2HCT exchanger CitP of lactic acid bacteria couples the

translocation of a single proton to the translocation of divalent $Hcit^{2-}$ or monovalent lac^-. In the physiological exchange mode, the ternary complex with bound $Hcit^{2-}$ moves from state "out" to "in," and that with bound lac^- moves from state "in" to "out" (step 3). During exchange, the proton is shuttled back and forward with no net transport. The transporter is optimized to catalyze exchange because the kinetics of isomerization of the ternary complex (step 3) are much faster than those of isomerization of the "unloaded" transporter (step 6) (94, 107). The latter step is omitted in the exchange reaction but is rate determining in the symport reaction. Movement of $Hcit^{2-}$ into the cell and lac^- out of the cell results in the generation of membrane potential. In the symport mode, CitP catalyzes electrogenic citrate transport and electroneutral lactate transport. If the transporter itself is neutral, the moving charge would be the net charge of the $H^+/Hcit^{2-}$ ion pair moving into the cell (steps 2, 3, and 4). If, on the other hand, the transporter itself is positively charged, the electrogenic step(s) would be directed outward and the charge would be carried by the H^+/lac^- ternary complex (steps 4, 3, and 2). In the latter case, the kinetics of electroneutral H^+/lac^- symport catalyzed by CitP may very well be dependent on the membrane potential. The forces driving the generation of the membrane potential in the exchange mode are the inwardly directed citrate or malate gradients and the outwardly directed lactate gradient maintained by the metabolism of the substrate inside the cell.

Antiport mechanism of CitS. An alternative kinetic mechanism was proposed for the Na^+-citrate transporter, CitS, of *K. pneumoniae* (109). The mechanism is based on the observed dimeric structure of the protein and is similar to the mechanism proposed for mitochondrial translocators. Mitochondrial transporters are antiporters that translocate a substrate in one direction and, obligatorily, couple transport of a second, structurally related substrate in the opposite direction. Well-known examples are the ATP/ADP translocator and the mitochondrial tricarboxylate carrier (102, 104). The transporters are homodimers, and each of the subunits contains a substrate binding site which faces the opposite side of the membrane (Fig. 10C). Reorientation of the binding site of one subunit is coupled to reorientation of the binding site on the other subunit (steps 5 and 6). At any given moment, half of the transporter has a binding site exposed to one or the other side of the membrane. Coupling between the inward and outward translocations in the dimer is warranted by the fact that isomerization is inhibited when only one of the two subunits has bound a substrate molecule (steps 1 and 2). Evidence for the antiport mechanism catalyzed by the CitS dimer was obtained in a kinetic study of purified CitS reconstituted in proteoliposomes. The rate of sodium motive force-driven citrate uptake in the proteoliposomes was dependent on the internal Na^+ concentration. It was proposed that the inward movement of $Hcit^{2-}$ and two Na^+ ions bound to one subunit in the dimer was coupled to the outward movement of one hydroxyl ion (OH^-) and one Na^+ ion bound to the other subunit. The mechanism accounts for the net translocation of one Na^+ ion, while the dependence of the initial rate on two external Na^+ ions is still maintained (76, 109, 135).

Alternate access. The kinetic states with the binding sites oriented to the two sides of the membrane correspond to different conformations of the transporter protein. The state with the binding sites exposed to the external medium corresponds to a conformation in which an aqueous pathway exists from the bulk water phase to the binding pocket on the surface of the protein. A similar pathway exists in the opposite orientation, but from the water phase at the other side of the membrane. The isomerization corresponds to a conformational change that blocks the pathway from one side of the membrane and, at the same time, opens up the pathway on the other side (Fig. 11). Important aspects of the alternate access model for substrate translocation were confirmed by the 3D crystal structures of the lactose transporter, LacY, and the glycerol-3-P/P_i exchanger, GlpT, which were crystallized with the substrate binding site facing the cytoplasm (2, 47). The model predicts that residues which are a part of or close to the substrate and co-ion binding sites should be accessible from both sides of the membrane, but never at the same time. Moreover, the properties of the access pathways are likely to be different at the two sides of the membrane. This is reflected in different affinities for substrate and co-ions in the two conformations. In the citrate/malate proton symporter, CimH, of *B. subtilis* and the Na^+/citrate symporter, CitS, of *K. pneumoniae*, cysteine residues in pore-loop Xa were shown to be accessible to membrane-impermeative reagents from both sides of the membrane in the absence of substrate, when the transporter can freely shift between the two conformations (Fig. 11, states 1 and 2; see "Membrane topology" in "STRUC TURE" above) (64, 135). Differences between the two conformations were demonstrated by locking the transporter in either conformation, which was achieved by adding substrate or co-ions at one side of the membrane. In the resulting binary complexes, the isomerization was blocked (see previous section). Binding of Na^+ to CitS from the periplasmic side (Fig. 11, state 3) resulted in complete protection of Cys414 against the thiol-modifying reagents, whereas binding of Na^+ from the cytoplasmic side (state 4) only marginally affected the reactivity of the same cysteine residue. Also, the differences between the citrate-locked states 7 and 8 could be demonstrated. At the periplasmic side (state 7), the reactivity of Cys398 was moderately reduced in the citrate-bound state compared to the free state (state 1). The concentration of citrate producing half of the effect was below 1 mM. In contrast, at the cytoplasmic face, a much stronger reduction of

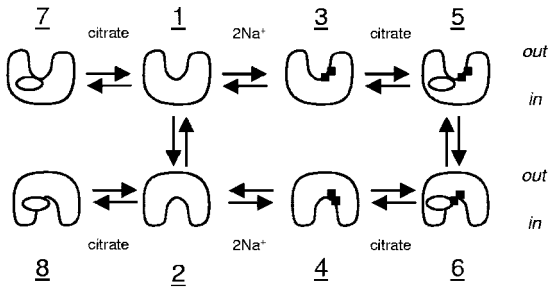

FIG. 11. Schematic representation of the alternate access model for substrate translocation in the symport mode of transport, based on CitS of *K. pneumoniae*. The protein can reorient the binding sites in the "unloaded" (states 1 and 2) and "fully loaded" (states 5 and 6) states. Reorientation is blocked in the citrate-bound (states 7 and 8) and Na+-bound (states 3 and 4) states. Symbols: ovals, citrate; squares, Na^+.

reactivity was observed, but concentrations of one order of magnitude higher were required to induce it. The accessibility of specific sites in the protein from both sides of the membrane and the different properties observed in the two major conformations of the transporter suggest a similar translocation mechanism for the 2HCT, LacY, and GlpT transporters.

In the antiporter mechanism for CitS of *K. pneumoniae* discussed above (109), at any time, half of the binding sites are exposed to one side of the membrane and the other half to the other side. However, a number of labeling experiments with CitS seem to indicate that the sites are all facing the same side of the membrane. A single-Cys mutant of the CitS protein embedded in the membrane was treated with a thiol reagent under different conditions, after which the residual free thiols were measured in detergent solution (135). (i) Treatment of CitS with a membrane-impermeative reagent from the cytoplasmic side of the membrane effectively labeled all Cys414 residues; (ii) in the citrate-bound state locked in the cytoplasmic orientation, Cys398 was completely protected against membrane-permeative *N*-ethylmaleimide; and (iii) in the Na^+-bound state locked in the cytoplasmic orientation, Cys398 was also completely protected against the same reagent. Even though alternative explanations may be given, the above observations argue against the antiporter mechanism for CitS as proposed by Pos and Dimroth (109).

Structure-Function Relationships

The conserved Arg in TMS XI. The best-conserved region in the 2HCT family is formed by the cytoplasmic loop between TMSs X and XI, containing pore-loop Xa and the cytoplasmic half of TMS XI (Fig. 5B). An arginine residue in TMS XI, positioned close to the membrane/cytoplasm interface, is the only residue with a charged side chain that is fully conserved in all members of the family (Fig. 9). Solid evidence has been obtained indicating that this residue is in direct contact with one of the carboxylate groups of the di- and tricarboxylate substrates of the transporters. Conservative replacement of the arginine residue at this position with a lysine residue in CitP of *Leuconostoc mesenteroides* (Arg425) and CimH of *B. subtilis* (Arg432) resulted in a lowering of the affinity of the transporters for citrate by one order of magnitude, while replacement with a cysteine residue reduced the affinity by at least two orders of magnitude (11, 64). The latter mutation, Arg428Cys, rendered CitS of *K. pneumoniae* inactive (J. S. Lolkema, unpublished data). The reduced affinity of the Arg-to-Lys mutants, in which the positive charge is retained, suggested an electrostatic interaction with one of the negatively charged carboxylate groups on the substrate. The reaction of the Arg-to-Cys mutants of CitP (10) and CimH (64) with the thiol reagent MTSEA (2-aminoethyl-methanethiosulfonate), which introduces a positive charge at the position of the cysteine residue, resulted in 50-fold and 2-fold increases of transport activity, respectively, while reaction with MTSES, which introduces a negative charge, resulted in a decrease of the activity. The activity of the Arg425Cys and Arg425Lys mutants of CitP could be further reduced by treatment with the thiol reagent PCMB (*p*-chloromercurybenzoate) and the lysine-specific reagent TNBS (2,4,6-trinitrobenzene sulfonate), respectively. In both cases, the modification was slowed down to some extent in the presence of high concentrations of substrate, suggesting that modifications at the position of the arginine residue do not prevent substrate binding but affect the affinity for the substrates.

A more detailed interaction between the arginine residue in TMS XI and the substrates follows from a binding site model that is based upon the substrate selectivity and, in particular, the stereoselectivity of the exchangers CitP and MleP of lactic acid bacteria (7, 9, 11). The transporters were shown to recognize a broad range of substrates, as long as they contained the 2-hydroxycarboxylate motif, i.e., $HO\text{-}CR_2\text{-}COO^-$, indicating specific and obligate interactions between sites on the protein and the carboxylate and hydroxyl groups on the substrate molecules (Fig. 12). At the same time, both transporters were quite tolerant towards the two R groups of the substrates (see "Transport properties" in "FUNCTION" above). However, a significant affinity difference was observed between di- and tricarboxylates and monocarboxylates, suggesting a specific interaction between a site on the protein and a carboxylate of one of the R groups. High affinity was observed only for the *S* enantiomers of dicarboxylates, while the *R* enantiomers behaved like monocarboxylate substrates. Arg425 in TMS XI was shown to be the residue in CitP that interacts with the carboxylate of the R group in the *S* enantiomeric configuration. In the exchange reaction, the affinity of the Arg425Lys mutant for (*S*)-malate was reduced from 90 μM to 1400 μM, while in the Arg425Cys mutant the affinity was reduced to undetectable levels (>10 mM). In contrast, the affinity for the monocarboxylate 2-hydroxyisobutyrate increased from 4.9 mM for the wild-type CitP to 1.2 mM for the Arg425Lys mutant and 0.22 mM for the Arg425Cys mutant. Clearly, Arg425 has a favorable interaction with the carboxylated R group in the *S* enantiomer of malate and an unfavorable interaction with a neutral R group (Fig. 12).

The carboxylate in the R group of (*S*)-malate and citrate that interacts with the Arg residue in TMS XI is the one that is removed in the decarboxylation steps in the malolactic and citrolactic fermentation pathways (see "Physiological function" in "FUNCTION" above). The interaction is therefore essential for the generation of the membrane potential and gives the transporters their high affinity for the substrate in the external medium and low affinity for the lactate product inside the cell. In one scenario, the positive charge of the arginine residues is compensated for by the negative charge of the carboxylate of the R group of (*S*)-malate (or citrate), making the inward-moving translocation electroneutral (Fig. 10B, step 3, up). In the outward-moving translocation (step 3, down) the charge is not compensated for by lactate, making this the electrogenic step.

Chimeras of CitP and MleP. The citrate/lactate exchanger CitP and malate/lactate exchanger MleP found in lactic acid bacteria share 48% sequence identity. Exchanging the 46 C-terminal residues containing (most of) pore-loop Xa and the conserved arginine residue in TMS XI between MleP and CitP did not alter the exchange kinetics with the di- and tricarboxylate substrates citrate and malate (10). The affinities of the chimeric transporters for citrate and malate were determined by the N-terminal parts of the proteins, indicating that the different interactions of the two transporters with citrate and malate are located there. The situation was different for monocarboxylate substrates such as mandelate and 2-hydroxy-

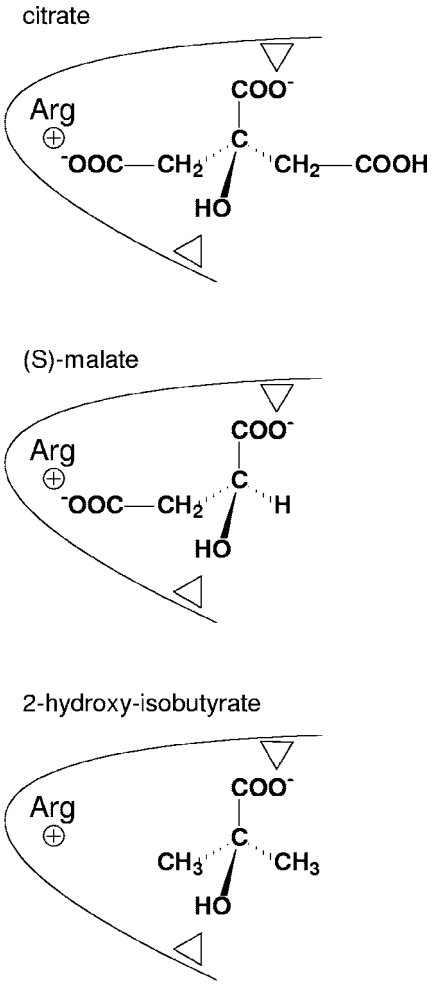

FIG. 12. Models for binding of tri-, di-, and monocarboxylates to 2HCT transporters. Open arrows point to the carboxylate and hydroxy groups of the 2-hydroxycarboxylate motif that is common to all substrates. The arrows represent essential interactions between the substrate molecules and binding site residues on the protein. Arg^+ represents the conserved arginine residue in TMS XI that interacts with a second carboxylate of citrate (top panel) and (*S*)-malate (middle panel), resulting in high affinity binding. Citrate binds in the divalent anionic state, and the protonated carboxylate group points away from the Arg residue. In the monocarboxylate 2-hydroxyisobutyrate, the interaction is not favorable, resulting in low-affinity binding (bottom panel).

isovalerate. Wild-type CitP cannot exchange (*S*)-malate for (*S*)-mandelate and (*S*)-2-hydroxybutyrate, while MleP can. The activity was associated with the C-terminal 46 residues (10). CitP acquired exchange activity when the C-terminal stretch was replaced by the corresponding part of MleP, while MleP lost the activity following the reverse replacement. The results are consistent with a direct interaction of sites in the C-terminal fragment with the monocarboxylate substrates and support the involvement of region Xa and TMS XI in the binding pocket and translocation pathway.

Interaction of substrate and co-ions with the Xa region. The pore-loop structure proposed for the Xa region is likely to be an essential feature in the translocation mechanism, and it is expected that mutations and chemical modifications of residues in the region affect the properties of the transporters. Cys398 and Cys414 are both in the predicted pore-loop of CitS of *K. pneumoniae*. Mutation of both endogenous cysteines to Ser did not affect the activity with respect to citrate (134), but modification of the residues by the alkylating agent *N*-ethylmaleimide significantly reduced the transport activity of the proteins. Cys414 was highly reactive towards the reagent (134, 135). Insertion of the 10-kDa biotin acceptor domain at the Cys398 position completely abolished activity. Interestingly, insertion of the same domain 10 residues upstream (Ile389), between TMS X and the pore-loop, was tolerated by the protein (146). Residues Arg420 and Gln428 are between the pore-loop and TMS XI of CimH of *B. subtilis*. Mutation of the residues to Cys did not affect transport activity, but treatment of the cysteine mutants with *N*-ethylmaleimide completely abolished uptake activity. The reactivity of the cysteine residue in Arg420Cys was significantly lower than that observed for the cysteine in Gln428Cys (64).

Binding of citrate to CitS of *K. pneumoniae* in the absence of Na^+ ions (Fig. 11, states 7 and 8) reduced the reactivity of Cys398 towards thiol reagents, while the effect on the reactivity of Cys414 was only marginal. Also for Cys398, the protection was far from complete at saturating concentrations of citrate, especially from the periplasmic side of the membrane (see above). This indicates that both residues may not be directly involved in binding of the substrate, but the bound substrate somehow obstructs the access pathway for the reagent to the residue (135). An analogous conclusion may be made for the Arg420-to-Cys and Gln428-to-Cys mutations in loop Xa of CimH of *B. subtilis*. While the affinity of the Arg420Cys mutant for citrate and malate was similar to that of wild type CimH, the presence of saturating concentrations of substrate protected the cysteine residue from reacting with different thiol reagents (64). Similarly, the Gln428Cys mutation did not alter the affinities for the substrates, but citrate protected against membrane-impermeative MTSES when added at the periplasmic side of the membrane. The accessibility pathway to Cys428 from the cytoplasmic side of the membrane was not affected.

Na^+ symporters have the advantage over H^+ symporters in that it is easier to study the interactions of the transporter with the co-ion. CitS of *K. pneumoniae* showed an obligate requirement for Na^+ and transported two Na^+ ions in symport with citrate, as evidenced by the sigmoidal increase of the rate of citrate transport with increasing Na^+ concentration (76, 135). Half of the maximal rate in the right-side-out membranes was obtained at an Na^+ concentration of 3 mM. The apparent affinity for Na^+ was two times lower in a mutant where the Cys414 in the pore-loop region Xa was mutated to Ser. A more drastic effect could be attributed to mutation Cys398Ser, which increased the apparent affinity constant to 28 mM. In both mutants, the sigmoidal relationship was retained, indicating that the transport stoichiometry was not affected. Binding of Na^+ to CitS in the absence of citrate was shown to have a significant effect on the conformation of the Xa region (134, 135). In the periplasmically oriented conformation of the Na^+-bound state (Fig. 11, state 3), Cys398 and Cys414 in the pore loop are not accessible for thiol reagents. Titration with increasing Na^+ ion concentrations revealed a sigmoidal increase of the protection, demonstrating that two Na^+ ions bound to CitS in the absence of citrate (134). In the opposite orientation

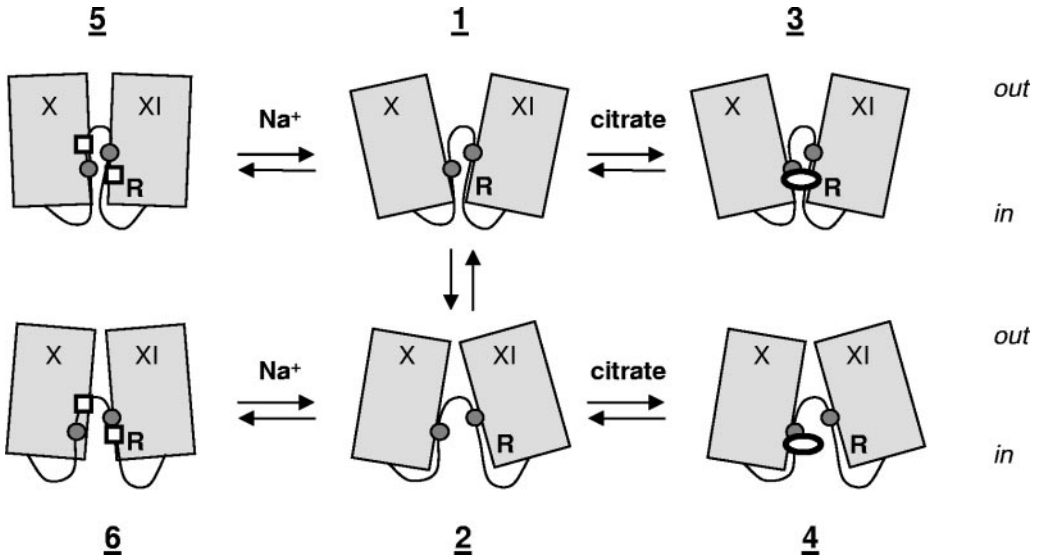

FIG. 13. Mechanistic model for the transporters of the 2HCT family. The scheme shows TMSs X and XI and pore-loop Xa in the C-terminal domain. States 1, 3, and 5 represent conformations of the protein with the binding site exposed to the external medium. States 2, 4, and 6 represent conformations with the binding site facing the cytoplasm. Isomerization of the two conformations is allowed only between states 1 and 2 and between the states that have bound both citrate and Na^+ (not shown in the model). See text for further explanation. Symbols: ovals, citrate; squares, Na^+ ions; circles, Cys residues; R, conserved arginine residue.

(state 4) and in the presence of saturating concentrations of Na^+, the accessibility of the two cysteine residues was reduced by different amounts depending on the reagent used (135).

While binding of citrate or Na^+ to CitS of *K. pneumoniae* resulted in various levels of protection (ranging from full to none) of the two endogenous cysteine residues in pore-loop Xa against thiol reagents, both residues were almost fully protected in the presence of both substrate and co-ion (134, 135). At concentrations of citrate and Na^+ ions that hardly affected the inactivation of the single-Cys CitS mutants in right-side-out membrane vesicles by N-ethylmaleimide and MTSET when present separately, the combination of both resulted in almost complete protection. This indicates that the conformation of the "ternary complexes" (Fig. 11, states 5 and 6) is different from that of the "binary complexes."

Mutations in the Vb region. Hydrophobic region Vb is predicted to contain a pore-loop region that enters the membrane-embedded part of the protein from the periplasmic side of the membrane (Fig. 9). Little information is available on the importance of this part of the protein for its function. A His tag inserted at a position between the pore-loop and TMS VI was tolerated by CitS of *K. pneumoniae* (146). The sequence motif GGxG that is conserved in the pore-loops (Fig. 7) is GGNG in the Vb region of CitS. Mutation of asparagine to valine in the motif reduced the affinity for citrate by one order of magnitude, suggesting that Asp185 could participate in binding of the substrate (56). Mutation of the glutamate residue Glu194 in the putative pore-loop had little effect on the overall kinetics of CitS (56).

Mechanistic Model

Based on the structural and functional data, the translocation site of the 2HCT transporters is built from two sets of transmembrane segments that are connected by pore-loops: TMSs V and VI connected by pore-loop Vb in the N-terminal domain and TMSs X and XI connected by Xa in the C-terminal domain (Fig. 9). The two sets have similar structures but are inserted with opposite orientation in the membrane. The two pore-loops may contact each other in the middle of the membrane. Since few data are available on the role of pore-loop Vb in the mechanism, the contribution to the translocation site of the N-terminal domain was removed in the model in Fig. 13. Taking CitS of *K. pneumoniae* as the paradigm for the 2HCT transporters, the two endogenous cysteine residues in pore-loop Xa are exposed alternately to the periplasmic and cytoplasmic sides of the membrane when the transporter changes the orientation of the binding sites (states 1 and 2). In the periplasmically exposed state, they are deeper in the pore, accessible only to small thiol reagents which can diffuse into the pore, while in the opposite orientation, molecules as large as AmdiS can reach the thiol groups. Essential to the proposed mechanism is the position of the substrate binding site at the membrane/cytoplasm interface. This follows from the position of the conserved residue Arg425 (CitP numbering), which is believed to be one of the residues that interacts with the substrate. The asymmetric positioning of the substrate binding site is different from the lactose transporter LacY and glycerol-3-P transporter GlpT, transporters of the MFS family, the Na^+/H^+ antiporter NhaA, and the leucine transporter LeuT, where the substrates/co-ions bind halfway into the membrane (2, 47, 49, 153). Important consequences of this position of the substrate binding site may be that (i) the pore is wider in the outward-facing conformation than in the case of LacY and GlpT and (ii) isomerization from the outward- to the inward-facing conformation (Fig. 13, states 1 to 2) may pull apart the sites on the protein that coordinate the substrate molecule, thereby disrupting the binding site. The latter mechanism would result in

significantly different affinities of the protein for the substrate at the two sides of the membrane. For CitS of *K. pneumoniae*, the data indicate that the protein binds citrate in the absence of Na^+ ions and both Na^+ ions in the absence of citrate, suggesting that the binding sites for substrate and co-ions are physically separated. Na^+ ion binding does not induce the citrate binding site, nor are they part of the citrate binding site. Consequently, the isomerization of the free transporter can be inhibited by binding of either citrate or Na^+ ions (Fig. 13, states 3, 4, 5 and 6). In the model, the pore-loop containing Cys398 and Cys414 of CitS protrudes into the pore beyond the citrate binding site (states 3 and 4), making them accessible for the small thiol reagents from the periplasm in the outward-facing conformation. The relative position of the binding site and the pore-loop explains the small effect or lack of effect of bound citrate on the accessibilities of Cys398 and Cys414, respectively. The much more effective protection of Cys398 in the inward-facing orientation by citrate indicates that Cys398 is close to the citrate binding site in the pore. Binding of Na^+ may result in partial closure of the pore in the outward-facing conformation (state 5), making it too narrow for the thiol reagents to enter. Since citrate is still able to bind in this situation, the effect of Na^+ binding functions as an increase in the specificity of the pore at the periplasmic side. In the inward-facing orientation, the protection by Na^+ binding is decreased, due to the location of the cysteine residues at the entrance of the pore (state 6). Finally, the "ternary complex" state of the transporters, in which both citrate and Na^+ ions are bound, may represent a conformation where the pore is closed at both sides of the membrane, leaving the two cysteine residues essentially inaccessible from the water phases. Possibly, the inward-facing and outward-facing conformations of the ternary complexes (represented by states 5 and 6) are very similar structures requiring only small changes to open up to either side of the membrane.

CONCLUSIONS

Transporters of the 2HCT family are found exclusively in the bacterial kingdom, predominantly in the class *Bacillales* of the phylum *Firmicutes* and the beta and gamma subdivisions of the phylum *Proteobacteria*, where they function in very specific niches. Occasionally members of this family have "crossed over" to other classes within the two phyla or even to other phyla, but these events appear to be rare. Genome sequences of bacteria outside the *Firmicutes* and *Proteobacteria* phyla will become available in the near future and will confirm these findings.

In their phylogenetic niche, the transporters of the 2HCT family are involved in related physiological functions. The characterized members are involved in the metabolism of the di- and tricarboxylates citrate and malate, mostly under fermentative conditions. They function in the uptake of the substrates from the medium, but in the malolactic and citrolactic fermentation pathways they also function in the excretion of the end products. Typical components of the pathways are the transporters and a decarboxylase for malate or oxaloacetate, the first intermediate in citrate fermentation. The "chemistries" of the pathways are similar, but there is remarkable flexibility in their implementation in terms of selecting transporters from different families, different types of decarboxylases, different energy-coupling mechanisms, and even different sensory systems for substrate detection. As a result, different combinations of transporters and decarboxylases, and decarboxylases of various subunit composition, are found in the genomes of related organisms (Tables 2 and 3). It looks like nature had a toolbox containing the tools suitable for the job and that different organisms took from it what became available at some point in evolution. All of these data support the notion that evolution is not a gradual process but that extensive mixing of fragments of DNA containing complete genes took place between organisms.

The great sequence diversity of secondary transporters suggests that the proteins developed independently of each other more than once during evolution. The notion is supported by the high-resolution structures that have recently become available. The drug transporter AcrB of *E. coli* (98), the lactose transporter LacY (2) and the glycerol-P/P_i exchanger GlpT (47) of *E. coli*, members of the major facilitator superfamily, the Na^+/H^+ antiporter NhaA of *E. coli* (49), the glutamate transporter homolog Glt_{Ph} of the archaeon *P. horikoshii* (154), the leucine transporter LeuT of *A. aeolicus* (153), and the mitochondrial ATP/ADP translocator (105) all reveal different folds and catalyze translocation by different mechanisms. Moreover, the structural and functional distinction between transporters and channels is challenged by the ammonia transporter AmtB of *E. coli*, a presumed secondary transporter which revealed a structure more reminiscent of a channel protein (61) and by the members of the chloride channel family, ClC, that are either Cl^-/H^+ antiporters or voltage-gated chloride channels (3, 106, 122). More 3D structures of secondary transporters are needed to determine the number of different folds, and more functional studies are needed to determine the number of different translocation mechanisms among the many transporter families that have been identified. The 2HCT family is likely to reveal yet another transporter structure and mechanism that may be representative of the 32 families in structural class ST[3] of the MemGen classification (79, 80). The antibody library recently obtained for CitS of *K. pneumoniae* may be helpful in determining its 3D structure (115).

ACKNOWLEDGMENTS

This work was supported by The Netherlands Organization for Scientific Research, NWO-CW, and by European Commission grant QLK1-CT-2002–02388.

REFERENCES

1. **Abe, K., Z. S. Ruan, and P. C. Maloney.** 1996. Cloning, sequencing, and expression in *Escherichia coli* of OxlT, the oxalate:formate exchange protein of *Oxalobacter formigens*. J. Biol. Chem. **271:**6789–6793.
2. **Abramson, J., I. Smirnova, V. Kasho, G. Verner, H. R. Kaback, and S. Iwata.** 2003. Structure and mechanism of the lactose permease of *Escherichia coli*. Science **301:**610–615.
3. **Accardi, A., and C. Miller.** 2004. Secondary active transport mediated by a prokaryotic homologue of ClC Cl− channels. Nature **427:**803–807.
4. **Altschul, S. F., T. L. Madden, A. A. Schaffer, J. Zhang, Z. Zhang, W. Miller, and D. J. Lipman.** 1997. Gapped BLAST and PSI-BLAST: a new generation of protein database search. Nucleic Acids Res. **25:**3389–3402.
5. **Anantharam, V., M. J. Allison, and P. C. Maloney.** 1989. Oxalate:formate exchange. The basis for energy coupling in Oxalobacter. J. Biol. Chem. **264:**7244–7250.
6. **Ansanay, V., S. Dequin, B. Blondin, and P. Barre.** 1993. Cloning, sequence and expression of the gene encoding the malolactic enzyme from *Lactococcus lactis*. FEBS Lett. **332:**74–80.
7. **Bandell, M., V. Anasay, N. Rachidi, S. Dequin, and J. S. Lolkema.** 1997. Membrane potential-generating malate (MleP) and citrate (CitP) trans-

porters of lactic acid bacteria are homologous proteins. Substrate specificity of the 2-hydroxycarboxylate transporter family. J. Biol. Chem. **272:**18140–18146.

8. **Bandell, M., M. E. Lhotte, C. M. Teysset, A. Veyrat, H. Prevost, V. Dartois, C. Divies, W. N. Konings, and J. S. Lolkema.** 1998. Mechanism of the citrate transporters in carbohydrate and citrate cometabolism in *Lactococcus* and *Leuconostoc* species. Appl. Environ. Microbiol. **64:**1594–1600.
9. **Bandell, M., and J. S. Lolkema.** 1999. Stereoselectivity of the membrane potential-generating citrate and malate transporters of lactic acid bacteria. Biochemistry **38:**10352–10360.
10. **Bandell, M., and J. S. Lolkema.** 2000. The conserved C-terminus of the citrate (CitP) and malate (MleP) transporters of lactic acid bacteria is involved in substrate recognition. Biochemistry **39:**13059–13067.
11. **Bandell, M., and J. S. Lolkema.** 2000. Arg-425 of the citrate transporter CitP is responsible for high affinity binding of di- and tricarboxylates. J. Biol. Chem. **275:**39130–39136.
12. **Bekal, S., J. van Beeuman, B. Samyn, D. Garmyn, S. Henini, S. Divies, and H. Prévost.** 1998. Purification of *Leuconostoc mesenteroides* citrate lyase and cloning and characterization of the *citCDEFG* gene cluster. J. Bacteriol. **180:**647–654.
13. **Bekal-Si Ali, S., C. Divies, and H. Prevost.** 1999. Genetic organization of the *citCDEF* locus and identification of *mae* and *clyR* genes from *Leuconostoc mesenteroides*. J. Bacteriol. **181:**4411–4416.
14. **Bott, M.** 1997. Anaerobic citrate metabolism and its regulation in enterobacteria. Arch. Microbiol. **167:**78–88.
15. **Bott, M., and P. Dimroth.** 1994. *Klebsiella pneumoniae* genes for citrate lyase and citrate lyase ligase: localization, sequencing, and expression. Mol. Microbiol. **14:**347–356.
16. **Bott, M., M. Meyer, and P. Dimroth.** 1995. Regulation of anaerobic citrate metabolism in *Klebsiella pneumoniae*. Mol. Microbiol. **18:**533–546.
17. **Busch, W., and M. H. Saier, Jr.** 2004. The IUBMB-endorsed transporter classification system. Mol. Biotechnol. **27:**253–262.
18. **Cogan, T. M.** 1981. Constitutive nature of the enzymes of citrate metabolism in *Streptococcus lactis subsp. diacetylactis*. J. Dairy Res. **48:**489–495.
19. **Cogan, T. M.** 1987. Co-metabolism of citrate and glucose by *Leuconostoc* spp.: effects on growth, substrates and products. J. Appl. Bacteriol. **63:**551–558.
20. **Connil, N., Y. Le Breton, X. Dousset, Y. Auffray, A. Rince, and H. Prevost.** 2002. Identification of the *Enterococcus faecalis* tyrosine decarboxylase operon involved in tyramine production. Appl. Environ. Microbiol. **68:**3537–3544.
21. **Consler, T. G., B. L. Persson, H. Jung, K. H. Zen, K. Jung, G. G. Prive, G. E. Verner, and H. R. Kaback.** 1993. Properties and purification of an active biotinylated lactose permease from *Escherichia coli*. Proc. Natl. Acad. Sci. USA **90:**6934–6938.
22. **Cronan, J. E., Jr.** 1990. Biotination of proteins in vivo. A post-translational modification to label, purify, and study proteins. J. Biol. Chem. **265:**10323–10333.
23. **Cselovszki, J., G. Wolf, and W. P. Hammes.** 1992. Production of formate, acetate and succinate by anaerobic fermentation of *Lactocobacillus pentosum* in the presence of citrate. Appl. Microbiol. Biotechnol. **37:**94–97.
24. **David, S., M. E. van der Rest, A. J. Driessen, G. Simons, and W. M. de Vos.** 1990. Nucleotide sequence and expression in *Escherichia coli* of the *Lactococcus lactis* citrate permease gene. J. Bacteriol. **172:**5789–5794.
25. **Davies, S. J., P. Golby, D. Omrani, S. A. Broad, V. L. Harrington, J. R. Guest, D. J. Kelly, and S. C. Andrews.** 1999. Inactivation and regulation of the aerobic (C4)-dicarboxylate transport (*dctA*) gene of *Escherichia coli*. J. Bacteriol. **181:**5624–5635.
26. **Denayrolles, M., M. Aigle, and A. Lonvaud-Funel.** 1994. Cloning and sequencing analysis of the gene encoding *Lactococcus lactis* malolactic enzyme: relationship with malic enzymes. FEMS Microbiol. Lett. **116:**79–86.
27. **de Ruyter, P. G., O. P. Kuipers, and W. M. de Vos.** 1996. Controlled gene expression systems for *Lactococcus lactis* with the food-grade inducer nisin. Appl. Environ. Microbiol. **62:**3662–3667.
28. **Di Berardino, M., and P. Dimroth.** 1995. Synthesis of the oxaloacetate decarboxylase Na+ pump and its individual subunits in *Escherichia coli* and analysis of their function. Eur. J. Biochem. **231:**790–801.
29. **Dimroth, P., and A. Thomer.** 1986. Citrate transport in *Klebsiella pneumoniae*. Biol. Chem. Hoppe Seyler **367:**813–823.
30. **Dimroth, P., and A. Thomer.** 1990. Solubilization and reconstitution of the Na(+)-dependent citrate carrier of *Klebsiella pneumoniae*. J. Biol. Chem. **265:**7221–7224.
31. **Dimroth, P., and A. Thomer.** 1993. On the mechanism of sodium ion translocation by oxaloacetate decarboxylase of *Klebsiella pneumoniae*. Biochemistry **32:**1734–1739.
32. **Ding, P. Z.** 2004. Loop X/XI, the largest cytoplasmic loop in the membrane-bound melibiose carrier of *Escherichia coli*, is a functional re-entrant loop. Biochim. Biophys. Acta **1660:**106–117.
33. **Doan, T., P. Servant, S. Tojo, H. Yamaguchi, G. Lerondel, K. Yoshida, Y. Fujita, and S. Aymerich.** 2003. The Bacillus subtilis ywkA gene encodes a malic enzyme and its transcription is activated by the YufL/YufM two-component system in response to malate. Microbiology **149:**2331–2343.
34. **Doyle, D. A., J. M. Cabral, R. A. Pfuetzner, A. Kuo, J. M. Gulbi, S. L. Cohen, B. T. Chait, and R. MacKinnon.** 1998. The structure of the potassium channel: molecular basis of K+ conduction and selectivity. Science **280:**69–77.
35. **Drider, D., S. Bekal, and H. Prevost.** 2004. Genetic organization and expression of citrate permease in lactic acid bacteria. Genet. Mol. Res. **3:**273–281.
36. **Driessen, A. J. M., W. de Vrij, and W. N. Konings.** 1985. Incorporation of beefheart cytochrome *c* oxidase as a proton motive force generating mechanism in bacterial membrane vesicles. Proc. Natl. Acad. Sci. USA **82:**7555–7559.
37. **Dutzler, R., E. B. Campbell, M. Cadene, B. T. Chait, and R. MacKinnon.** 2002. X-ray structure of a ClC chloride channel at 3.0 Å reveals the molecular basis of anion selectivity. Nature **415:**287–294.
38. **Eisenberg, D., R. M. Weiss, and T. C. Terwilliger.** 1982. The helical hydrophobic moment: a measure of the amphiphilicity of a helix. Nature **299:**371–374.
39. **Fu, D., A. Libson, L. J. Miercke, C. Weitzman, P. Nollert, J. Krucinski, and R. M. Stroud.** 2000. Structural determinants of water permeation through aquaporin-1. Science **290:**481–486.
40. **García-Quintáns, N., C. Magni, D. de Mendoza, and P. López.** 1998. The citrate transport system of *Lactococcus lactis* subsp. *lactis* biovar diacetylactis is induced by acid stress. Appl. Environ. Microbiol. **64:**850–857.
41. **Golby, P., S. Davies, D. J. Kelly, J. R. Guest, and S. C. Andrews.** 1999. Identification and characterization of a two-component sensor-kinase and response-regulator system (DcuS-DcuR) controlling gene expression in response to C4-dicarboxylates in *Escherichia coli*. J. Bacteriol. **181:**1238–1248.
42. **Grunewald, M., A. Bendahan, and B. I. Kanner.** 1998. Biotinylation of single cysteine mutants of the glutamate transporter GLT-1 from rat brain reveals its unusual topology. Neuron **21:**623–632.
43. **Grunewald, M., and B. I. Kanner.** 2000. The accessibility of a novel reentrant loop of the glutamate transporter GLT-1 is restricted by its substrate. J. Biol. Chem. **275:**9684–9689.
44. **Heidelberg, J. F., J. A. Eisen, W. C. Nelson, R. A. Clayton, M. L. Gwinn, R. J. Dodson, D. H. Haft, E. K. Hickey, J. D. Peterson, L. Umayam, S. R. Gill, K. E. Nelson, T. D. Read, H. Tettelin, D. Richardson, M. D. Ermolaeva, J. Vamathevan, S. Bass, H. Qin, I. Dragoi, P. Sellers, L. McDonald, T. Utterback, R. D. Fleishmann, W. C. Nierman, and O. White.** 2000. DNA sequence of both chromosomes of the cholera pathogen *Vibrio cholerae*. Nature **406:**477–483.
45. **Henderson, P. J., and M. C. Maiden.** 1990. Homologous sugar transport proteins in *Escherichia coli* and their relatives in both prokaryotes and eukaryotes. Philos. Trans. R. Soc. London B **326:**391–410.
46. **Heymann, J. A., R. Sarker, T. Hirai, D. Shi, J. L. Milne, P. C. Maloney, and S. Subramaniam.** 2001. Projection structure and molecular architecture of OxlT, a bacterial membrane transporter. EMBO J. **20:**4408–4413.
47. **Huang, Y., M. J. Lemieux, J. Song, M. Auer, and D.-N. Wang.** 2003. Structure and mechanism of the glycerol-3-phosphate transporter from *Escherichia coli*. Science **301:**616–620.
48. **Hugenholtz, J.** 1993. Citrate metabolism in lactic acid bacteria. FEMS Microbiol. Rev. **12:**165–178.
49. **Hunte, C., E. Screpanti, M. Venturi, A. Rimon, E. Padan, and H. Michel.** 2005. Structure of the Na^+/H^+ antiporter and insight into mechanism of action and regulation by pH. Nature **435:**1197–1202.
50. **Ishiguro, N., H. Izawa, M. Shinagawa, T. Shimamoto, and T. Tsuchiya.** 1992. Cloning and nucleotide sequence of the gene (citC) encoding a citrate carrier from several *Salmonella serovars*. J. Biol. Chem. **267:**9559–9564.
51. **Iwamoto, T., A. Uehara, I. Imanaga, and M. Shigekawa.** 2000. The Na+/Ca2+ exchanger NCX1 has oppositely oriented reentrant loop domains that contain conserved aspartic acids whose mutation alters its apparent Ca2+ affinity. J. Biol. Chem. **275:**38571–38580.
52. **Jack, D. L., I. T. Paulsen, and M. H. Saier.** 2000. The amino acid/polyamine/organocation (APC) superfamily of transporters specific for amino acids, polyamines and organocations. Microbiology **146:**1797–1814.
53. **Jack, D. L., N. M. Yang, and M. H. Saier, Jr.** 2001. The drug/metabolite transporter superfamily. Eur. J. Biochem. **268:**3620–3639.
54. **Janausch, I. G., E. Zientz, Q. H. Tran, A. Kröger, and G. Unden.** 2002. C4-dicarboxylate carriers and sensors in bacteria. Biochim. Biophys. Acta **1553:**39–56.
55. **Kaback, H. R.** 1971. Bacterial membranes. Methods Enzymol. **22:**99–120.
56. **Kästner, C. N., P. Dimroth, and K. M. Pos.** 2000. The Na+-dependent citrate carrier of *Klebsiella pneumoniae*: high-level expression and site-directed mutagenesis of asparagine-185 and glutamate-194. Arch. Microbiol. **174:**67–73.
57. **Kästner, C. N., M. Prummer, B. Sick, A. Renn, U. P. Wild, and P. Dimroth.** 2003. The citrate carrier CitS probed by single-molecule fluorescence spectroscopy. Biophys. J. **84:**1651–1659.
58. **Kästner, C. N., K. Schneider, P. Dimroth, and K. M. Pos.** 2002. Characterization of the citrate/acetate antiporter CitW of *Klebsiella pneumoniae*. Arch. Microbiol. **177:**500–506.
59. **Kawai, S., H. Suzuki, K. Yamamoto, M. Inui, H. Yukawa, and H. Kumagai.** 1996. Purification and characterization of a malic enzyme from the ruminal

bacterium *Streptococcus bovis* ATCC 15352 and cloning and sequencing of its gene. Appl. Environ. Microbiol. **62:**2692–2700.
60. **Kawai, S., H. Suzuki, K. Yamamoto, and H. Kumagai.** 1997. Characterization of the L-malate permease gene (*maeP*) of *Streptococcus bovis* ATCC 15352. J. Bacteriol. **179:**4056–4060.
61. **Khademi, S., J. O'Connell III, J. Remis, Y. Robles-Colmenares, L. J. W. Miercke, and R. Stroud.** 2004. Mechanism of ammonia transport by Amt/MEP/Rh: structure of AmtB at 1.35 A. Science **305:**1587–1594.
62. **Krogh, A., B. Larsson, G. von Heijne, and E. L. Sonnhammer.** 2001. Predicting transmembrane protein topology with a hidden Markov model: application to complete genomes. J. Mol. Biol. **305:**567–580.
63. **Krom, B. P., R. Aardema, and J. S. Lolkema.** 2001. *Bacillus subtilis* YxkJ is a secondary transporter of the 2-hydroxycarboxylate transporter family that transports L-malate and citrate. J. Bacteriol. **183:**5862–5869.
64. **Krom, B. P., and J. S. Lolkema.** 2003. Conserved residues R420 and Q428 in a cytoplasmic loop of the citrate/malate transporter CimH of *Bacillus subtilis* are accessible from the external face of the membrane. Biochemistry **42:**467–474.
65. **Krom, B. P., J. B. Warner, W. N. Konings, and J. S. Lolkema.** 2000. Complementary metal ion specificity of the metal-citrate transporters CitM and CitH of *Bacillus subtilis*. J. Bacteriol. **182:**6374–6381.
66. **Krom, B. P., J. B. Warner, W. N. Konings, and J. S. Lolkema.** 2003. Transporters involved in uptake of di- and tricarboxylates in *Bacillus subtilis*. Antonie Leeuwenhoek **84:**69–80.
67. **Kunji, E. R., D. J. Slotboom, and B. Poolman.** 2003. *Lactococcus lactis* as host for overproduction of functional membrane proteins. Biochim. Biophys. Acta **1610:**97–108.
68. **Kyte, J., and R. F. Doolittle.** 1982. A simple method for displaying the hydropathic character of a protein. J. Mol. Biol. **157:**105–132.
69. **Labarre, C., C. Diviés, and J. Guzzo.** 1996. Genetic organization of the *mle* locus and identification of a *mleR*-like gene from *Leuconostoc oenos*. Appl. Environ. Microbiol. **62:**4493–4498.
70. **Labarre, C., J. Guzzo, J. F. Cavin, and C. Divies.** 1996. Cloning and characterization of the genes encoding the malolactic enzyme and the malate permease of *Leuconostoc oenos*. Appl. Environ. Microbiol. **62:**1274–1282.
71. **Lambert, G., I. C. Forster, G. Stange, K. Kohler, J. Biber, and H. Murer.** 2001. Cysteine mutagenesis reveals novel structure-function features within the predicted third extracellular loop of the type IIa Na(+)/P(i) cotransporter. J. Gen. Physiol. **117:**533–546.
72. **Lindgren, S. E., L. T. Axelsson, and R. F. McFeeters.** 1990. Anaerobic L-lactate degradation by *Lactobacillus plantarum*. FEMS Microbiol. Lett. **66:**209–214.
73. **Liu, S. Q.** 2002. A review: malolactic fermentation in wine—beyond deacidification. J. Appl. Microbiol. **92:**589–601.
74. **Liu, D., W. E. Karsten, and P. F. Cook.** 2000. Lysine 199 is the general acid in the NAD-malic enzyme reaction. Biochemistry **39:**11955–11960.
75. **Lo, T. Y. C., M. K. Rayman, and B. D. Sanwal.** 1972. Transport of succinate in *Escherichia coli*. I. Biochemical and genetic studies of transport in whole cells. J. Biol. Chem. **247:**6323–6331.
76. **Lolkema, J. S., H. Enequist, and M. E. van der Rest.** 1994. Transport of citrate catalyzed by the sodium-dependent citrate carrier of *Klebsiella pneumoniae* is obligatorily coupled to the transport of two sodium ions. Eur. J. Biochem. **220:**469–475.
77. **Lolkema, J. S., B. Poolman, and W. N. Konings.** 1995. Role of scalar protons in metabolic energy generation in lactic acid bacteria. J. Bioenerg. Biomembr. **27:**467–473.
78. **Lolkema, J. S., B. Poolman, and W. N. Konings.** 1996. Secondary transporters and metabolic energy generation in bacteria, p. 229–260. *In* W. N. Konings, H. R. Kaback, and J. S. Lolkema (ed.), Handbook of biological physics. Elsevier Science, Amsterdam, The Netherlands.
79. **Lolkema, J. S., and D. J. Slotboom.** 1998. Estimation of structural similarity of membrane proteins by hydropathy profile alignment. Mol. Membr. Biol. **15:**33–42.
80. **Lolkema, J. S., and D. J. Slotboom.** 2003. Classification of 29 families of secondary transport proteins into a single structural class using hydropathy profile analysis. J. Mol. Biol. **327:**901–909.
81. **Lolkema, J. S., and D. J. Slotboom.** 2005. Sequence and hydropathy profile analysis of two classes of secondary transporters. Mol. Membr. Biol. **22:**177–189.
82. **Lolkema, J. S., I. Sobczak, and D. J. Slotboom.** 2005. Secondary transporters of the 2HCT family contain two homologous domains with inverted membrane topology and *trans* re-entrant loops. FEBS J. **272:**2334–2344.
83. **Lonvaud-Funel, A.** 2001. Biogenic amines in wines: role of lactic acid bacteria. FEMS Microbiol. Lett. **199:**9–13.
84. **Lopez de Felipe, F. L., C. Magni, D. de Mendoza, and P. López.** 1995. Citrate utilization gene cluster of the *Lactococcus lactis biovar diacetylactis*: organization and regulation of expression. Mol. Gen. Genet. **246:**590–599.
85. **Lopez de Felipe, F. L., C. Magni, D. de Mendoza, and P. López.** 1996. Transcriptional activation of the citrate permease P gene of *Lactococcus lactis biovar diacetylactis* by an insertion sequence-like element present in plasmid pCIT264. Mol. Gen. Genet. **250:**428–436.
86. **Lucas, P., J. Landete, M. Coton, E. Coton, and A. Lonvaud-Funel.** 2003. The tyrosine decarboxylase operon of *Lactobacillus brevis* IOEB 9809: characterization and conservation in tyramine-producing bacteria. FEMS Microbiol. Lett. **229:**65–71.
87. **Lucas, P. M., W. M. Wolken, O. Claisse, J. S. Lolkema, and A. Lonvaud-Funel.** 2005. A histamine-producing pathway encoded on an unstable plasmid in *Lactobacillus hilgardii* 0006. Appl. Environ. Microbiol. **71:**1417–1424.
88. **Magni, C., F. L. de Felipe, P. López, and D. de Mendoza.** 1996. Characterization of an insertion sequence-like element identified in plasmid pCIT264 from *Lactococcus lactis subsp. lactis biovar diacetylactis*. FEMS Microbiol. Lett. **136:**289–295.
89. **Magni, C., D. de Mendoza, W. N. Konings, and J. S. Lolkema.** 1999. Mechanism of citrate metabolism in *Lactococcus lactis*: resistance against lactate toxicity at low pH. J. Bacteriol. **181:**1451–1457.
90. **Manoil, C., and J. Beckwith.** 1986. A genetic approach to analyzing membrane protein topology. Science **233:**1403–1408.
91. **Martín, M., M. A. Corrales, D. de Mendoza, P. López, and C. Magni.** 1999. Cloning and molecular characterization of the citrate utilization citMCDEFGRP cluster of *Leuconostoc paramesenteroides*. FEMS Microbiol. Lett. **174:**231–238.
92. **Martín, M., C. Magni, P. López, and D. de Mendoza.** 2000. Transcriptional control of the citrate-inducible *citMCDEFGRP* operon, encoding genes involved in citrate fermentation in *Leuconostoc paramesenteroides*. J. Bacteriol. **182:**3904–3912.
93. **Martín, M., P. D. Sender, S. Peirú, D. de Mendoza, and C. Magni.** 2004. Acid-inducible transcription of the operon encoding the citrate lyase complex of *Lactococcus lactis* biovar diacetylactis CRL264. J. Bacteriol. **186:**5649–5660.
94. **Marty-Teysset, C., J. S. Lolkema, P. Schmitt, C. Divies, and W. N. Konings.** 1995. Membrane potential-generating transport of citrate and malate catalyzed by CitP of *Leuconostoc mesenteroides*. J. Biol. Chem. **270:**25370–25376.
95. **Marty-Teysset, C., J. S. Lolkema, P. Schmitt, C. Divies, and W. N. Konings.** 1996. The citrate metabolic pathway in *Leuconostoc mesenteroides*: expression, amino acid synthesis, and alpha-ketocarboxylate transport. J. Bacteriol. **178:**6209–6215.
96. **Marty-Teysset, C., C. Posthuma, J. S. Lolkema, P. Schmitt, C. Divies, and W. N. Konings.** 1996. Proton motive force generation by citrolactic fermentation in *Leuconostoc mesenteroides*. J. Bacteriol. **178:**2178–2185.
97. **Molenaar, D., J. S. Bosscher, B. ten Brink, A. J. Driessen, and W. N. Konings.** 1993. Generation of a proton motive force by histidine decarboxylation and electrogenic histidine/histamine antiport in *Lactobacillus buchneri*. J. Bacteriol. **175:**2864–2870.
98. **Murakami, S., R. Nakashima, E. Yamashita, and A. Yamaguchi.** 2002. Crystal structure of bacterial multidrug efflux transporter AcrB. Nature **419:**587–593.
99. **Murata, K., K. Mitsuoka, T. Hirai, T. Walz, P. Agre, J. B. Heymann, A. Engels, and Y. Fujiyoshi.** 2000. Structural determinants of water permeation through aquaporin-1. Nature **407:**599–605.
100. **Nicoll, D. A., M. Ottolia, L. Lu, Y. Lu, and K. D. Philipson.** 1999. A new topological model of the cardiac sarcolemmal Na+-Ca2+ exchanger. J. Biol. Chem. **274:**910–917.
101. **Otto, R., R. G. Lageveen, H. Veldkamp, and Konings, W. N.** 1982. Lactate efflux-induced electrical potential in membrane vesicles of *Streptococcus cremoris*. J. Bacteriol. **149:**733–738.
102. **Palmieri, F.** 2004. The mitochondrial transporter family (SLC25): physiological and pathological implications. Pflugers Arch. Eur. J. Physiol. **447:**689–709.
103. **Paulsen, I. T., M. K. Sliwinski, and M. H. Saier, Jr.** 1998. Microbial genome analyses: global comparisons of transport capabilities based on phylogenies, bioenergetics and substrate specificities. J. Mol. Biol. **277:**573–592.
104. **Pebay-Peyroula, E., and G. Brandolin.** 2004. Nucleotide exchange in mitochondria: insight at a molecular level. Curr. Opin. Struct. Biol. **14:**420–425.
105. **Pebay-Peyroula, E., C. Dahout-Gonzalez, R. Kahn, V. Trezeguet, G. J. Lauquin, and G. Brandolin.** 2003. Structure of mitochondrial ADP/ATP carrier in complex with carboxyatractyloside. Nature **426:**39–44.
106. **Picollo, A., and M. Pusch.** 2005. Chloride/proton antiporter activity of mammalian CLC proteins ClC-4 and ClC-5. Nature **436:**420–423.
107. **Poolman, B., D. Molenaar, E. J. Smid, T. Ubbink, T. Abee, P. P. Renault, and W. N. Konings.** 1991. Malolactic fermentation: electrogenic malate uptake and malate/lactate antiport generate metabolic energy. J. Bacteriol. **173:**6030–6037.
108. **Pos, K. M., M. Bott, and P. Dimroth.** 1994. Purification of two active fusion proteins of the Na(+)-dependent citrate carrier of *Klebsiella pneumoniae*. FEBS Lett. **347:**37–41.
109. **Pos, K. M., and P. Dimroth.** 1996. Functional properties of the purified Na(+)-dependent citrate carrier of *Klebsiella pneumoniae*: evidence for asymmetric orientation of the carrier protein in proteoliposomes. Biochemistry **35:**1018–1026.
110. **Pos, K. M., P. Dimroth, and M. Bott.** 1998. The *Escherichia coli* citrate carrier CitT: a member of a novel eubacterial transporter family related to

the 2-oxoglutarate/malate translocator from spinach chloroplasts. J. Bacteriol. **180:**4160–4165.
111. **Prakash, S., G. Cooper, S. Singhi, and M. H. Saier, Jr.** 2003. The ion transporter superfamily. Biochim. Biophys. Acta **1618:**79–92.
112. **Qiu, Z., D. A. Nicoll, and K. D. Philipson.** 2001. Helix packing of functionally important regions of the cardiac Na(+)-Ca(2+) exchanger. J. Biol. Chem. **276:**194–199.
113. **Reizer, J., A. Reizer, and M. H. Saier, Jr.** 1994. A functional superfamily of sodium/solute symporters. Biochim. Biophys. Acta **1197:**133–166.
114. **Renault, P., C. Gaillardin, and H. Heslot.** 1989. Product of the *Lactococcus lactis* gene required for malolactic fermentation is homologous to a family of positive regulators. J. Bacteriol. **171:**3108–3114.
115. **Röthlisberger, D., K. M. Pos, and A. Plückthun.** 2004. An antibody library for stabilizing and crystallizing membrane proteins—selecting binders to the citrate carrier CitS. FEBS Lett. **564:**340–348.
116. **Sääf, A., L. Baars, and G. von Heijne.** 2001. The internal repeats in the Na+/Ca2+ exchanger-related *Escherichia coli* protein YrbG have opposite membrane topologies. J. Biol. Chem. **276:**18905–18907.
117. **Saier, M. H.** 2000. A functional-phylogenetic classification system for transmembrane solute transporters. Microbiol. Mol. Rev. **64:**354–411.
118. **Saier, M. H., Jr., J. T. Beatty, A. Goffeau, K. T. Harley, W. H. Heijne, S. C. Huang, D. L. Jack, P. S. Jahn, K. Lew, J. Liu, S. S. Pao, I. T. Paulsen, T. T. Tseng, and P. S. Virk.** 1999. The major facilitator superfamily. J. Mol. Microbiol. Biotechnol. **1:**257–279.
119. **Salema, M., J. S. Lolkema, M. V. San Romao, and M. C. Lourero Dias.** 1996. The proton motive force generated in *Leuconostoc oenos* by L-malate fermentation. J. Bacteriol. **178:**3127–3132.
120. **Salema, M., B. Poolman, J. S. Lolkema, M. C. Dias, and W. N. Konings.** 1994. Uniport of monoanionic L-malate in membrane vesicles from *Leuconostoc oenos*. Eur. J. Biochem. **225:**289–295.
121. **Salou, P., P. Loubiere, and A. Pareilleux.** 1994. Growth and energetics of *Leuconostoc oenos* during cometabolism of glucose with citrate or fructose. Appl. Environ. Microbiol. **60:**1459–1466.
122. **Scheel, O., A. A. Zdebik, S. Lourdel, and T. J. Jentsch.** 2005. Voltage-dependent electrogenic chloride/proton exchange by endosomal CLC proteins. Nature **436:**424–427.
123. **Schmitt, P., and C. Divies.** 1991. Co-metabolism of citrate and lactose by *Leuconostoc mesenteroides subsp. cremoris*. J. Ferment. Bioeng. **71:**72–74.
124. **Schneider, K., P. Dimroth, and M. Bott.** 2000. Biosynthesis of the prosthetic group of citrate lyase. Biochemistry **39:**9438–9450.
125. **Schneider, K., C. N. Kästner, M. Meyer, M. Wessel, P. Dimroth, and M. Bott.** 2002. Identification of a gene cluster in *Klebsiella pneumoniae* which includes *citX*, a gene required for biosynthesis of the citrate lyase prosthetic group J. Bacteriol. **184:**2439–2446.
126. **Schwarz, E., and D. Oesterhelt.** 1985. Cloning and expression of *Klebsiella pneumoniae* genes coding for citrate transport and fermentation. EMBO J. **4:**1599–1603.
127. **Schwarz, E., D. Oesterhelt, H. Reinke, K. Beyreuther, and P. Dimroth.** 1988. The sodium ion translocating oxalacetate decarboxylase of *Klebsiella pneumoniae*. Sequence of the biotin-containing alpha-subunit and relationship to other biotin-containing enzymes. J. Biol. Chem. **263:**9640–9645.
128. **Seligman, L., and C. Manoil.** 1994. An amphipathic sequence determinant of membrane protein topology. J. Biol. Chem. **269:**19888–19896.
129. **Sender, P. D., M. G. Martín, S. Peirú, and C. Magni.** 2004. Characterization of an oxaloacetate decarboxylase that belongs to the malic enzyme family. FEBS Lett. **570:**217–222.
130. **Sesma, F., D. Gardiol, A. P. de Ruiz Holgado, and D. de Mendoza.** 1990. Cloning of the citrate permease gene of *Lactococcus lactis* subsp. *lactis* biovar diacetylactis and expression in *Escherichia coli*. Appl. Environ. Microbiol. **56:**2099–2103.
131. **Simmons, J. S.** 1926. A culture medium for differentiating organisms of typhoidcodon aerogenes and for isolating of certain fungi. J. Infect. Dis. **39:**209–214.
132. **Slotboom, D. J., W. N. Konings, and J. S. Lolkema.** 2001. Glutamate transporters combine transporter- and channel-like features. Trends Biochem. Sci. **26:**534–539.
133. **Slotboom, D. J., I. Sobczak, W. N. Konings, and J. S. Lolkema.** 1999. A conserved serine-rich stretch in the glutamate transporter family forms a substrate-sensitive reentrant loop. Proc. Natl. Acad. Sci. USA **96:**14282–14287.
134. **Sobczak, I., and J. S. Lolkema.** 2003. Accessibility of cysteine residues in a cytoplasmic loop of CitS of *Klebsiella pneumoniae* is controlled by the catalytic state of the transporter. Biochemistry **42:**9789–9796.
135. **Sobczak, I., and J. S. Lolkema.** 2004. Alternate access and a pore-loop structure in the Na^+-citrate transporter CitS of *Klebsiella pneumoniae*. J. Biol. Chem. **279:**31113–31120.
136. **Sobczak, I., and J. S. Lolkema.** 2005. Loop VIII/IX of the Na^+-citrate transporter CitS of *Klebsiella pneumoniae* folds into an amphipathic surface helix. Biochemistry **44:**5461–5470.
137. **Sobczak, I., and J. S. Lolkema.** 2005. Structural and mechanistic diversity of secondary transporters. Curr. Opin. Struct. Biol. **8:**161–167.
138. **Starenburg, M. J. C., and J. Hugenhooltz.** 1991. Citrate fermentation by *Lactococcus* and *Leuconostoc* spp. Appl. Environ. Microbiol. **57:**3535–3540.
139. **Takami, H., K. Nakasone, Y. Takaki, G. Manno, R. Sasaki, N. Masui, F. Fuji, C. Hirama, Y. Nakamura, N. Ogasawara, S. Kurara, and K. Horikoshi.** 2000. Complete genome sequence of the alkaliphilic bacterium *Bacillus halodurans* and genomic sequence comparison with *Bacillus subtilis*. Nucleic Acids Res. **28:**4317–4331.
140. **Tanaka, K., K. Kobayashi, and N. Ogasawara.** 2003. The Bacillus subtilis YufLM two-component system regulates the expression of the malate transporters MaeN (YufR) and YflS, and is essential for utilization of malate in minimal medium. Microbiology **149:**2317–2329.
141. **Thompson, J. D., D. G. Higgins, and T. J. Gibson.** 1994. CLUSTAL W: improving the sensitivity of progressive multiple sequence alignment through sequence weighting, position-specific gap penalties and weight matrix choice. Nucleic Acids Res. **22:**4673–4680.
142. **van der Rest, M. E., D. Molenaar, and W. N. Konings.** 1992. Mechanism of Na^+-dependent citrate transport in *Klebsiella pneumoniae*. J. Bacteriol. **174:**4893–4898.
143. **van der Rest, M. E., R. M. Siewe, T. Abee, E. Schwarz, D. Oesterhelt, and W. N. Konings.** 1992. Nucleotide sequence and functional properties of a sodium-dependent citrate transport system from *Klebsiella pneumoniae*. J. Biol. Chem. **267:**8971–8976.
144. **van Geest, M., and J. S. Lolkema.** 1996. Membrane topology of the sodium ion-dependent citrate carrier of *Klebsiella pneumoniae*. Evidence for a new structural class of secondary transporters. J. Biol. Chem. **271:**25582–25589.
145. **van Geest, M., and J. S. Lolkema.** 1999. Transmembrane segment (TMS) VIII of the Na(+)/Citrate transporter CitS requires downstream TMS IX for insertion in the *Escherichia coli* membrane. J. Biol. Chem. **274:**29705–29711.
146. **van Geest, M., and J. S. Lolkema.** 2000. Membrane topology of the Na(+)/citrate transporter CitS of *Klebsiella pneumoniae* by insertion mutagenesis. Biochim. Biophys. Acta **1466:**328–338.
147. **van Geest, M., and J. S. Lolkema.** 2000. Membrane topology and insertion of membrane proteins: search for topogenic signals. Microbiol. Mol. Biol. Rev. **64:**13–33.
148. **van Geest, M., I. Nilsson, G. von Heijne, and J. S. Lolkema.** 1999. Insertion of a bacterial secondary transport protein in the endoplasmic reticulum membrane. J. Biol. Chem. **274:**2816–2823.
149. **Vaughan, E. E., S. David, A. Harrington, C. Daly, G. F. Fitzgerald, and W. M. de Vos.** 1995. Characterization of plasmid-encoded citrate permease (*citP*) genes from *Leuconostoc* species reveals high sequence conservation with the *Lactococcus lactis citP* gene. Appl. Environ. Microbiol. **61:**3172–3176.
150. **Veenhoff, L. M., E. H. M. L. Heuberger, H. H. Duurkens, and B. Poolman.** 2001. Oligomeric state of membrane transport proteins analyzed with blue native electrophoresis and analytical ultracentrifugation. J. Mol. Biol. **317:**591–600.
151. **Wei, Y., A. Guffanti, M. Ito, and T. A. Krulwich.** 2000. *Bacillus subtilis* YqkI is a novel malic/Na+-lactate antiporter that enhances growth on malate at low protonmotive force. J. Biol. Chem. **275:**30287–30292.
152. **Wild, M. R., K. M. Pos, and P. Dimroth.** 2003. Site-directed sulfhydryl labeling of the oxaloacetate decarboxylase Na+ pump of *Klebsiella pneumoniae*: helix VIII comprises a portion of the sodium ion channel. Biochemistry **42:**11615–11624.
153. **Yamashita, A., S. K. Singh, T. Kawate, Y. Jin, and E. Gouaux.** 2005. Crystal strucutre of a bacterial homologue of Na^+/Cl^--dependent neurotransmitter transporters. Nature **437:**215–223.
154. **Yernool, D., O. Boudker, Y. Jin, and E. Gouaux.** 2004. Structure of a glutamate transporter homologue from *Pyrococcus horikoshii*. Nature **431:**811–818.